Table Ⅱ-3- 9 Key Points for the Design of Mineral Processing Tests (Proposal)

Test item	SAMPLE	Period
		0 2 4 6 8 10 12 14 16 MONTH
1. MINERALOGICAL STUDY		—
2. FLOATATION(BENCH SCALE)	200~500 kg	——
3. LEACHING(COLUMN TEST)	2~ 6 ton	——
4. FLOWSHEET DEVELOPMENT		——
5. PRE-FEASIBILITY STUDY		——

3-4-15 Proposal of Future Dressing Test Schedule

The outline of the dressing test necessary for the future is shown in Table II-3-9. First, mineralogical study is needed.

Although this is performed as the content of geological survey, the study from the standpoint of dressing usually covers further detailed areas and requires other special research.

Next, the basic test for flotation test is required. For mainly copper sulfide ore, dressing reagent, grinding grain and other flotation condition are selected to obtain an optimal dressing result. Mixed ore often requires a further wide research. The required amount of ore samples representative of a mineral deposit for this test and the forth test is 200 to 500 kg. As this sample, use of remaining specimen in the boring core or ores collected by large diameter boring can be considered.

Third, leaching test for copper oxide ore is required. In this test, the measurement of the relationship between the size and exudation, and acid consumption and the evaluation of accumulated impurities accompanied with the return of leaching solution are performed. The required amount of ore sample is probably 2 to 6 tons although it differs depending on the size of the column. Although this sample is desired to be picked up from the top of a mineral deposit, collecting it from a small mine in the neighborhood according to the result of sufficient mineralogical consideration can be considered.

Fourth, a test to consider and confirm a synthetic dressing flowsheet according to the above result is needed. On this stage, some idea such processing of mixed ore first and reprocessing of tailing by agitation leaching is considered to make a basic design most advantageous from synthetic viewpoints.

Fifth, PRE-F/S is performed according to the above matter. On this stage, it is necessary to make a test to obtain the design data of important machines (mill, thickener, filter). It takes at least 10 months up to this stage.

Sixth, a pilot plant test of the scale necessary for testifying PRE-F/S is carried out. In this case, two cases can be considered, that is, the case of building a pilot plant on site and the case of using an existing facility such as a research center. If an existing facility is used, the time needed up to the final F/S is estimated to be about six months if the procedure is performed with good steps.

CHAPTER 4 GEOPHYSICAL EXPLORATION

4-1 IP LOGGING

As the drill holes for IP logging, 10 drill holes were selected in order to reevaluate and reanalyze the abnormal sources which were detected at ENAMI's surface geophysical exploration (frequency-domain IP method, magnetic exploration) of last fiscal year.

The positions of the drill holes and the related work amounts are shown in Fig. II-4-1 and Table II-4-1 respectively.

4-1-1 MEASURING METHOD

The layout of the equipment for logging is shown in Fig. II-4-2. In order to prevent falling in of the hole wall in the surface layer, we inserted vinyl chloride casing into most of the 10 drill holes selected for logging. The outline of the measuring system is shown in Fig. II-4-3. Three electrodes were arranged as C - P - P from the end with intervals of 5 m. In order to prevent electromagnetic coupling, twisted pair cable was used for electric potential wire, and the current line was shielded. Since the level of the groundwater was low in general, before performing the following measurement we artificially raised the water level by using a tank lorry. The amount of water supply was around 1 ton at maximum.

The measuring procedure is as follows:

(1) Lower the cable to reach the depth for measurement.

(2) Send 3 Hz constant current from the transmitter.

(3) Measure electric potential.

(4) Transmit 0.3 Hz constant current.

(5) Read PFE value directly from the meter.

(6) Calculate the apparent resistivity value.

(7) Examine the data quality. In case the data are undesirable, repeat the procedure from (2) to (6).

(8) Repeat from (1) to (7) until the measurement of the final depth is completed.

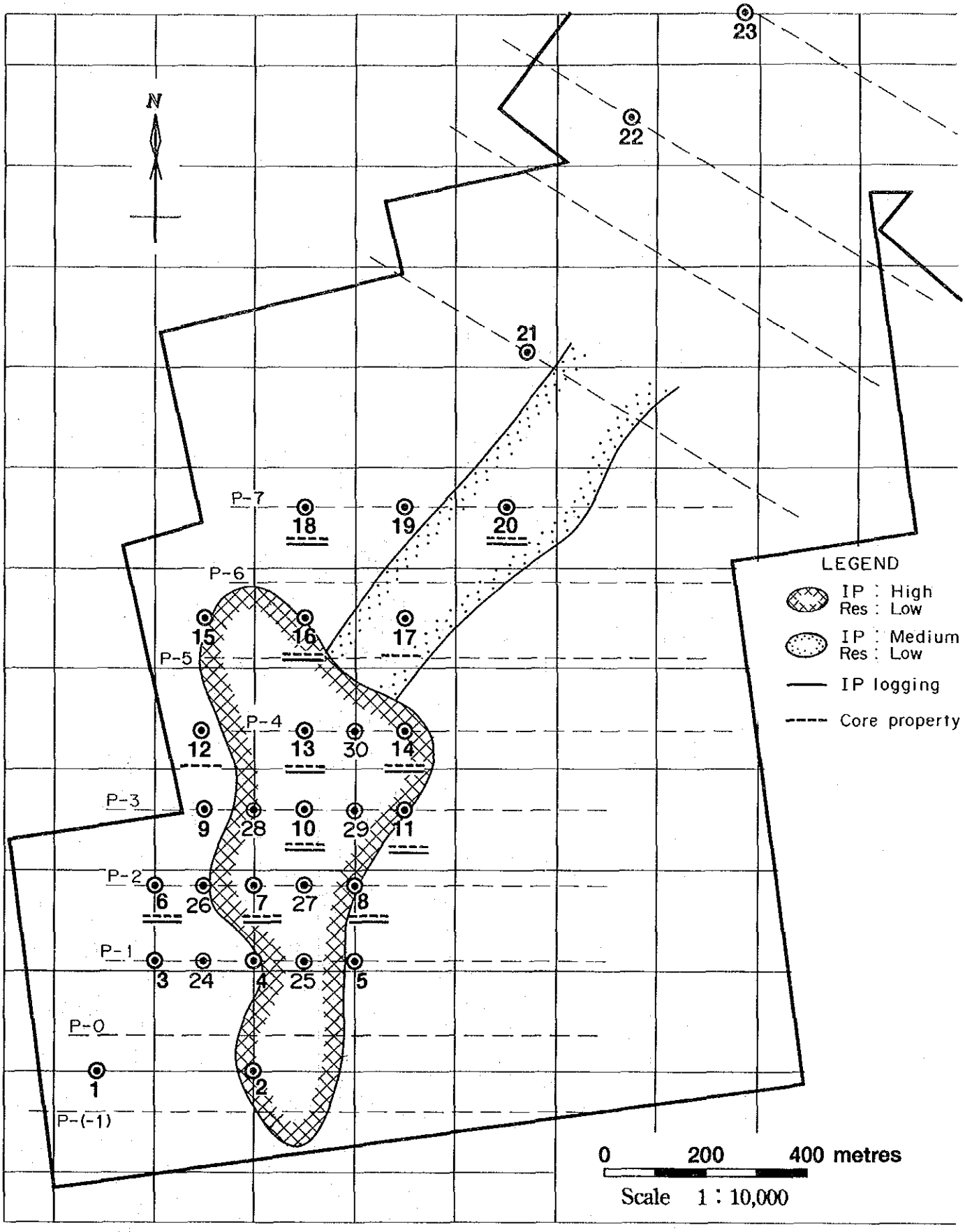

Fig. II-4- 1 Position map for IP logging

Table Ⅱ-4-1 List of works

Drill Hole	Depth	IP logging		IP Measurement of core samples		Magnetic susceptibility of core samples	
	(m)	Range (m)	Count	Range (m)	Count	Range (m)	Count
MJCC- 6	161.35	25 ~ 120	20	6.32 ~ 159.51	32	6.32 ~ 159.51	32
MJCC- 7	200.10	10 ~ 190	37	1.40 ~ 199.96	39	1.40 ~ 199.96	41
MJCC- 8	190.20	15 ~ 180	34	4.20 ~ 189.72	38	4.20 ~ 189.72	38
MJCC-10	160.40	5 ~ 150	30	0.77 ~ 159.83	33	0.77 ~ 159.83	33
MJCC-11	190.85	15 ~ 185	35	0.64 ~ 189.70	39	0.64 ~ 189.70	39
MJCC-12	169.30			13.00 ~ 165.15	31	4.90 ~ 165.15	33
MJCC-13	240.00	10 ~ 225	44	50.70 ~ 239.70	20	0.10 ~ 239.70	49
MJCC-14	204.90	10 ~ 195	38	0.32 ~ 204.61	42	0.32 ~ 204.61	42
MJCC-16	216.75	15 ~ 190	36	5.50 ~ 214.63	42	1.10 ~ 214.63	44
MJCC-17	160.05			0.44 ~ 160.00	33	0.44 ~ 160.00	33
MJCC-18	184.35	10 ~ 140	27	5.70 ~ 179.63	36	5.70 ~ 179.63	36
MJCC-20	187.65	10 ~ 185	36	1.10 ~ 184.95	26	1.10 ~ 184.95	38
				Standard samples	13		
Total	2265.9	1635	337	2157.3	424	2220.4	458

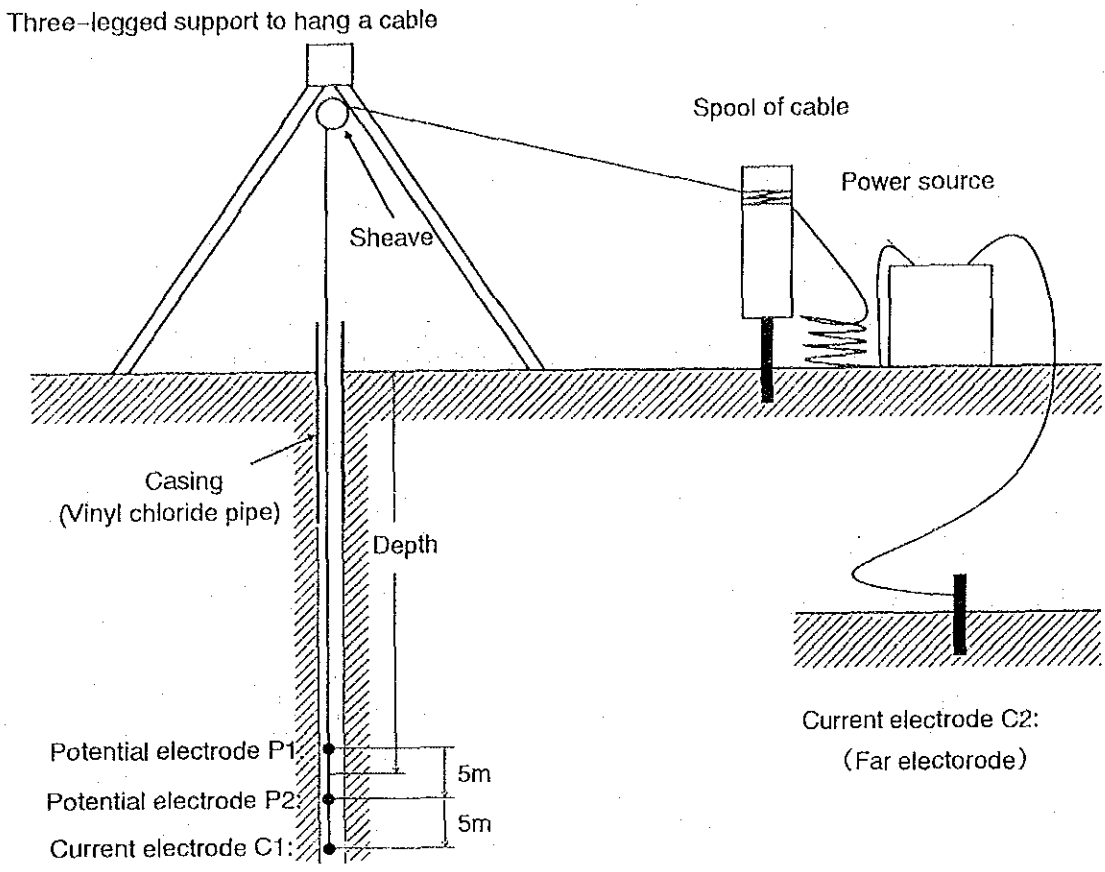

Fig. Ⅱ-4- 2 General idea for IP logging

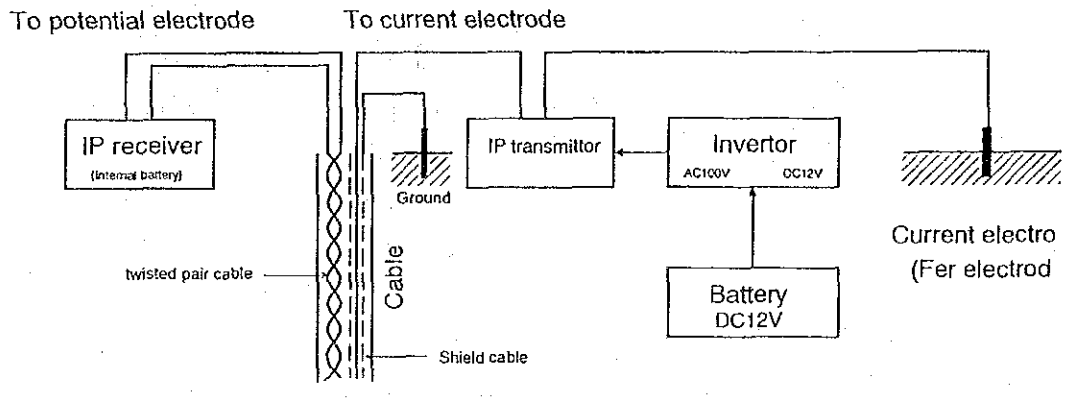

Fig. Ⅱ-4- 3 General idea for measurement system of IP logging

4-1-2 Equipment and materials for measurement

The equipment and materials used for this survey are as shown in the following Table II-4-2:

Table II-4-2 Measurement Equipment/Materials for IP Logging

Name of Equipment	Type of Equipment	Function/Performance
IP Transmitter	MODEL DH-125 Transmitter (Mfd. by Chiba Denshi K.K.)	Frequency Transmitted : 3.0, 1.0, 0.3, 0.1Hz, TD (2Sec) Output Current : 2, 5, 10, 20, 50, 75, 100, 125mA Power Supply : (AC 100V, 50 to 400Hz)
IP Receiver	(Frequency-domain) MODEL CH-8104R (Mfd. by Chiba Denshi K.K.)	Frequency Received : 3.0, 1.0, 0.3, 0.1Hz Input Level : 0.1mV to 10.0V Power Supply : 006P (9V) x 2
	(Time-domain) MK III (Mfd. by Hanteck Co., Canada)	Frequency Received : 2Sec Input Level : 30 μ V to 10V Power Supply : 12V battery
DC-AC Inverter	MODEL 1311 (Mfd. by Chiba Denshi K.K.)	Input : DC12.5V, 12Amax Output : AC100V, 1A
Cable for Logging	350m, 9 ϕ 3 cores { 2 cores: parallel twisted cable, 1 core : shielded cable Electrode intervals to be adjusted: C1 - P2 = P2 - P1 = 5m	

4-1-3 Measurement Results

Prior to measurement, relative measurement was performed in frequency-domain (F.D.) and time-domain (T.D.) at MJCC-14 in order to evaluate the influence of magnetic coupling on IP logging in F.D. The measurement results and the correlation diagram for the IP and resistivity values are shown in Fig. II-4-4 and Fig. II-4-5 respectively.

From these figures, we noted a certain relationship of primary recursiveness between the measured values of F.D. and T.D. without being influenced by electromagnetic coupling. Accordingly, we employed F.D. in our subsequent measurement as specified. The trial drilling for IP logging was performed at ten drill holes, i.e. MJCC-6, 7, 8, 10, 11, 13, 14, 16, 18 and 20, with a view to utilizing them for reanalysis of abnormal surface IP and to grasping the general tendency of the district surveyed. The locations of the drill holes for the geophysical logging are shown in Fig. II-4-1. The average of the measured values for each drill hole is shown in Table II-4-3. The results for each drill hole are as follows:

(MJCC-6): Fig. II-4-6

The average IP value for the depth from 0 to 100m is 12.0%, while the IP value for the depth from 100m to the hole bottom is a little higher indicating 8.8%. A similar tendency of an increase in values for deeper portions is noted also for resistivity. The lower resistivity values for the depth from 0 to 50m seem to have been influenced by decomposition of soil into clay.

(MJCC-7): Fig. II-4-7

The average IP value for the depth from 0m to the hole bottom is 13.5% which is high in general. Resistivity for the depth from 120 to 150m is 1 to 10m which is very low corresponding with an ore-forming zone of magnetized matter. Resistivity values for other depth are higher, indicating 100 to 1,000 Ω·m.

(MJCC-8): Fig. II-4-8

The average IP value for the depth from 0m to the hole bottom is 4.3% which is low in general, while that for the depth from 160 to 180m is a little higher indicating approx. 10%. Resistivity for the depth from 0m to the hole bottom is 363 Ω·m which is high in general with little variety.

(MJCC-10): Fig. II-4-9

The average IP value for the depth from 0m to the hole bottom is 17.6% which is high in general, keeping harmony with the existence of an ore-forming zone of sulfide. Resistivity of below 10 Ω·m is very low corresponding with an ore-forming zone of sulfide. Resistivities for other depth are high indicating 100 to 500 Ω·m.

(MJCC-11): Fig. II-4-10

The average IP value of 10.1% for the depth from 0m to the hole bottom is rather high, while that for the depth from 60 to 100m is especially high indicating around 15%. Resistivities for higher IP of 60 to 100m are rather low indicating 10 to 50 Ω·m, while those for other depth are around 100

Ω·m.

(MJCC-13): Fig. II-4-12

The average IP value for the depth from 0m to the hole bottom is 18.3% which is the highest value of all the results obtained by trial drilling of this time. The IP value for the depth from 20 to 80m is especially high indicating around 20% in correspondence with an ore-forming zone of sulfide. Resistivities for some portions are low indicating around 20 Ω·m. For the portion of 100m and deeper, both the resistivities and the IP value are high indicating around 1,000 Ω·m and around 20% respectively.

(MJCC-14): Fig. II-4-13

The average IP value for the depth from 0m to the hole bottom is 11.9% which shows a general tendency of rather high IP value. While resistivities for the depth from 0 to 100m are constant indicating around 200 Ω·m, those for the portion of 100m and deeper vary widely between 40 to 1,000 Ω·m.

(MJCC-16): Fig. II-4-14

While the average IP value of 3.0% is low for the depth from 0m to the hole bottom, that for the portion of 90m and deeper is rather high indicating around 5%. The resistivities for the depth from 0m to 100m are virtually constant indicating around 200 Ω·m, but those for the portion of 150m and deeper are very high indicating 1,000 to 10,000 Ω·m.

(MJCC-18): Fig. II-4-16

The average IP value for the depth from 0m to the hole bottom is 1.0% which is the lowest of all the results of this survey. While the resistivities of 10 to 100 Ω·m for the depth from 10 to 40m are rather low, those for the portion of 50m and deeper vary little indicating 100 to 300 Ω·m.

(MJCC-20): Fig. II-4-17

The average IP value of 3.5% for the depth from 0m to the hole bottom is low in general. While the resistivities for the depth from 0 to 120m are low in general indicating approx. 100 Ω·m, those for the depth from 130 to 180 m are higher indicating around 1,000 Ω·m.

4-2 Physical property Measurement for drill core

In this survey, we measured the magnetic susceptibility and IP effect means of core samples . In addition, IP values were measured for the standard pure samples of chalcopyrite, magnetite, specularite and hematite.

4-2-1 Measuring method

*** Magnetic susceptibility**

Core sampling was performed at intervals of 5m in principle. Broken cores was crushed and placed in acrylic cases for measurement. The measuring procedure is as follows:

(1) Initialize a magnetic susceptibility meter. (Off-set, zero-balance)

(2) Place the samples in coils, keep them balanced by adjusting the range and control, and record the readings in a field notebook.

(3) Take out the samples from the coils and measure the average length and diameter with calipers.

(4) Calculate the magnetic susceptibility applying a calculation formula (peculiar to the magnetic susceptibility meter).

*** IP effect**

The samples were prepared by parallel cutting for 5cm long each. Broken cores were excluded. Fig. II-4-18 shows the measurement system. The measuring procedure is as follows:

(1) Let the cut-out samples soak in water for one night.

(2) Measure the length and diameter of the samples.

(3) Set the samples in IP measuring equipment.

(4) Send 3Hz constant current from the transmitter.

(5) Measure electric potential.

(6) Transmit 0.3Hz constant current.

(7) Read PFE value directly from the meter.

(8) Calculate the apparent resistivity.

(9) Check the quality of the data obtained and repeat from (4) to (8) if necessary.

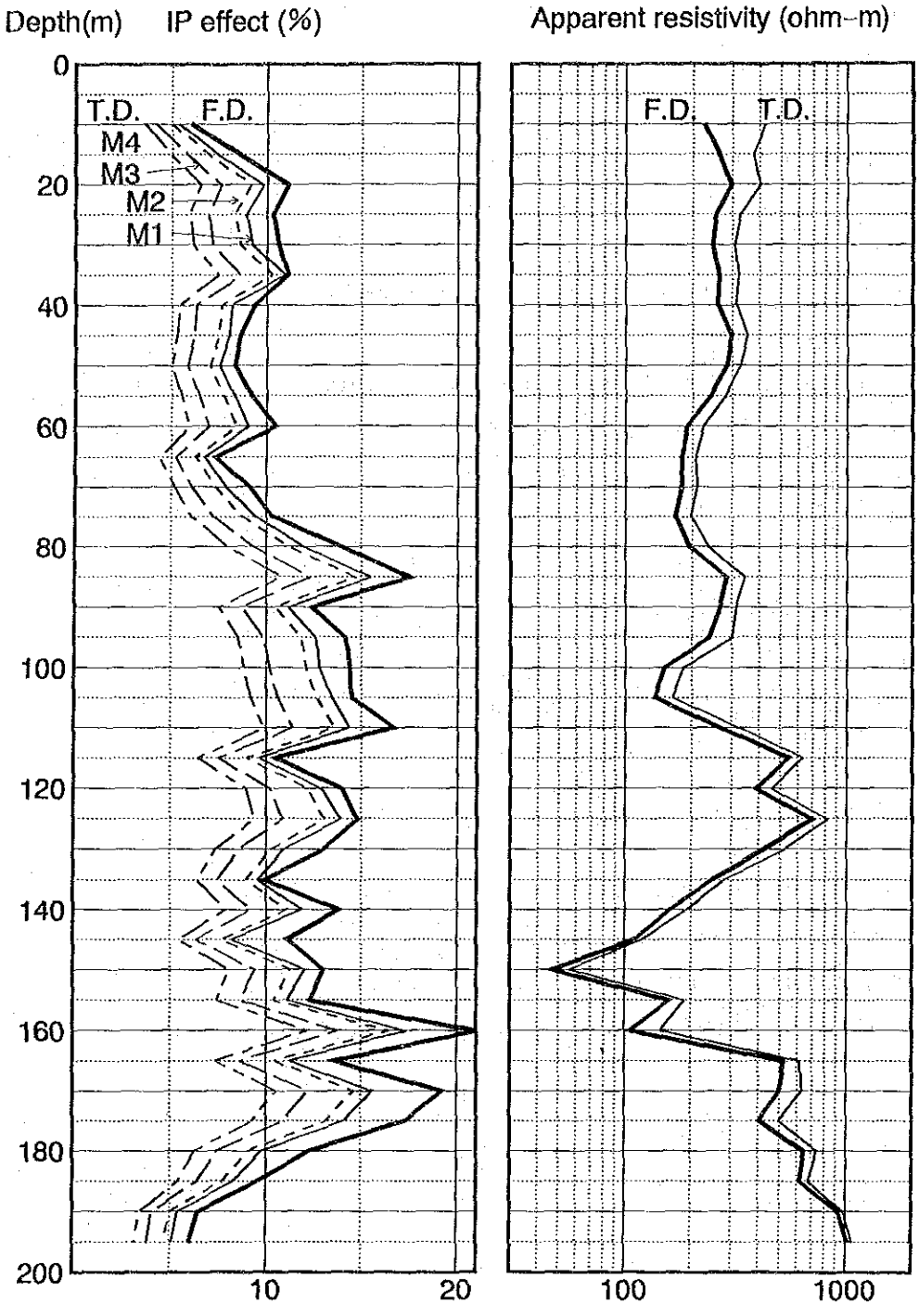

Fig. Ⅱ-4- 4 Comparative mesurement for Time Domain with Frequency Domain

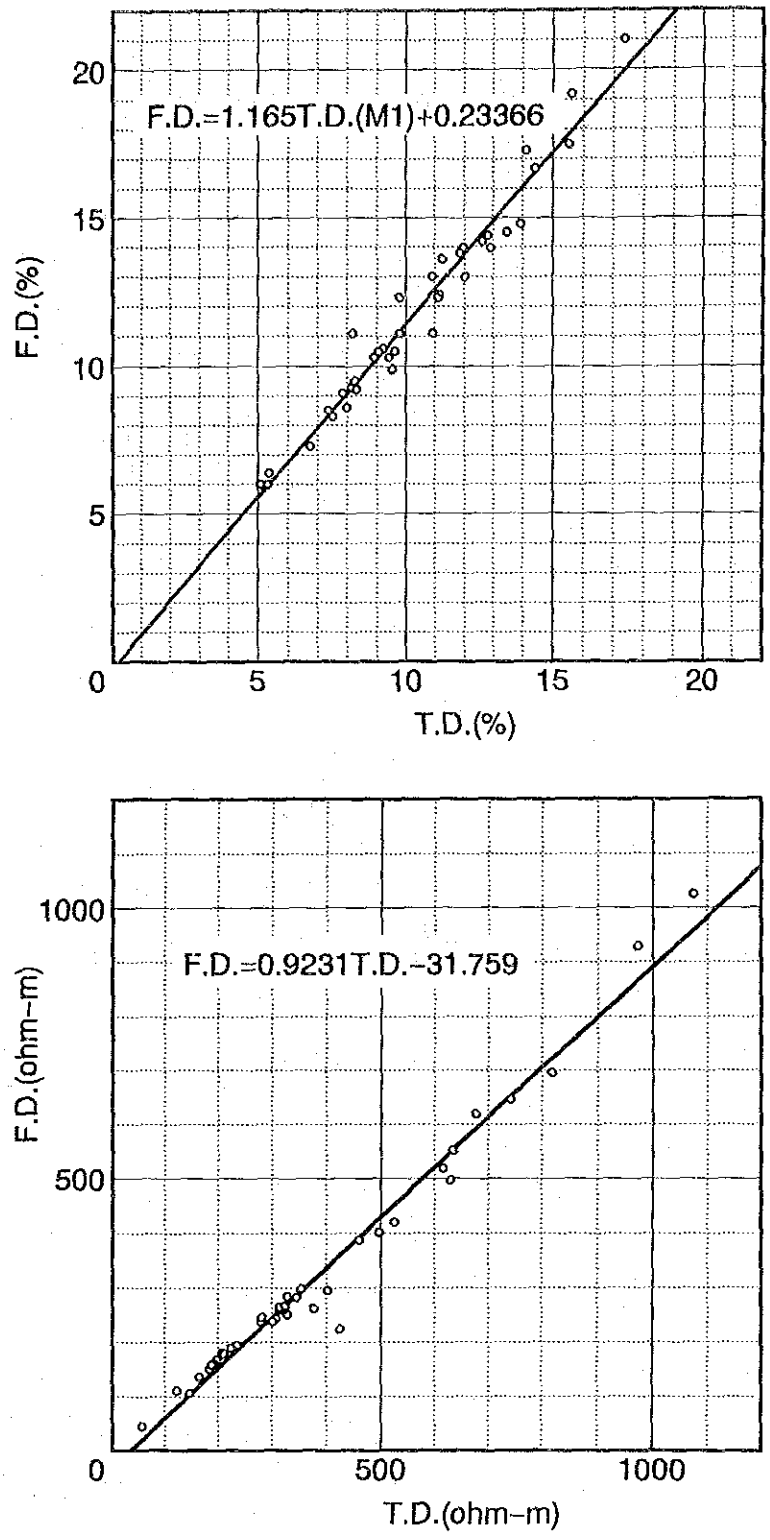

Fig. Ⅱ-4- 5 Correlation of Time and Frequency Domain

Table Ⅱ-4-3 List of the average geophysical properties in each hole

Content	Depth (m)	MJCC- 6	MJCC- 7	MJCC- 8	MJCC-10	MJCC-11	MJCC-12	MJCC-13	MJCC-14	MJCC-16	MJCC-17	MJCC-18	MJCC-20
Sample	Whole	3.1	22.0	2.2	30.2	14.2	3.1	25.3	10.4	2.9	4.5	1.4	2.2
IP effect	0～100	1.3	10.2	1.8	32.7	19.8	1.7	18.5	8.2	0.8	4.4	1.3	2.2
(%)	100～END	6.1	33.1	2.6	25.8	7.7	5.1	28.2	12.6	4.7	4.6	1.5	2.2
* Sample	Whole	256	313	259	169	190	109	1,606	618	220	1,996	226	444
Resistivity	0～100	102	359	203	86	276	76	451	363	53	1,239	255	181
(Ω・m)	100～END	1,188	275	341	545	123	180	2,768	1,055	718	4,600	194	860
Sample	Whole	3,119	9,071	6,649	24,605	2,908	3,037	23,125	8,735	5,404	4,738	2,157	3,475
Magnetic sus.	0～100	2,547	3,161	5,669	21,997	2,819	804	6,648	3,046	2,251	2,274	2,349	2,760
(10E-6 cgs)	100～END	4,073	14,700	7,629	29,168	3,001	6,472	34,488	13,906	8,031	8,529	1,916	4,269
Sample	Whole	12.6	1080	10.1	3210	270	328	591	37	49.5	5.11	9.31	11.3
Metal Factor	0～100	16.9	36.3	11.9	4620	431	80.8	1120	35.7	23.2	7.46	6.51	21.3
(10E-3 %/Ω・m)	100～END	5.4	2070	8.11	740	81.7	671	364	38.3	71.3	0.993	12.8	3.86
Logging	Whole	4.3	13.5	4.3	17.6	10.1		18.3	11.9	3.0		1.0	3.5
IP effect	0～100	2.0	11.0	3.2	15.8	11.3		16.9	10.5	1.6		1.0	2.7
(%)	100～END	8.8	15.8	5.4	20.6	8.9		19.4	13.2	4.3		1.2	4.4
* Logging	Whole	103	116	363	55	97		315	271	105		124	239
Resistivity	0～100	64	264	340	28	99		155	237	26		112	104
(Ω・m)	100～END	423	53	388	169	95		515	305	373		150	553
Logging	Whole	15.5	951	13.2	706	220		123	55.4	47.6		8.86	20.7
Metal Factor	0～100	12.1	41.7	9.15	935	274		238	44.5	54.5		8.87	26.6
(10E-3 %/Ω・m)	100～END	22.2	1810	17.3	312	169		43.8	65.2	41.4		8.83	14.7
Fe content	Whole	15.6	28.6	18.1	29.1	28.4	7.8	19.9	23.6	10.1	14.8	7.9	22.8
	0～100	15.6	30.9	19.5	33.2	32.9	5.8	24.1	27.8	9.1	17.1	7.2	24.9
(%)	100～END	15.6	26.4	16.7	22.5	23.7	10.6	17.0	19.8	10.9	11.1	8.6	20.6
Cu content	Whole	0.09	0.26	0.11	0.35	0.12	0.23	0.16	0.13	0.14	0.11	0.03	0.20
(Insoluble)	0～100	0.09	0.15	0.15	0.46	0.10	0.13	0.29	0.14	0.17	0.17	0.02	0.25
(%)	100～END	0.07	0.36	0.06	0.17	0.15	0.37	0.07	0.12	0.12	0.01	0.04	0.15

*:Geometric mean

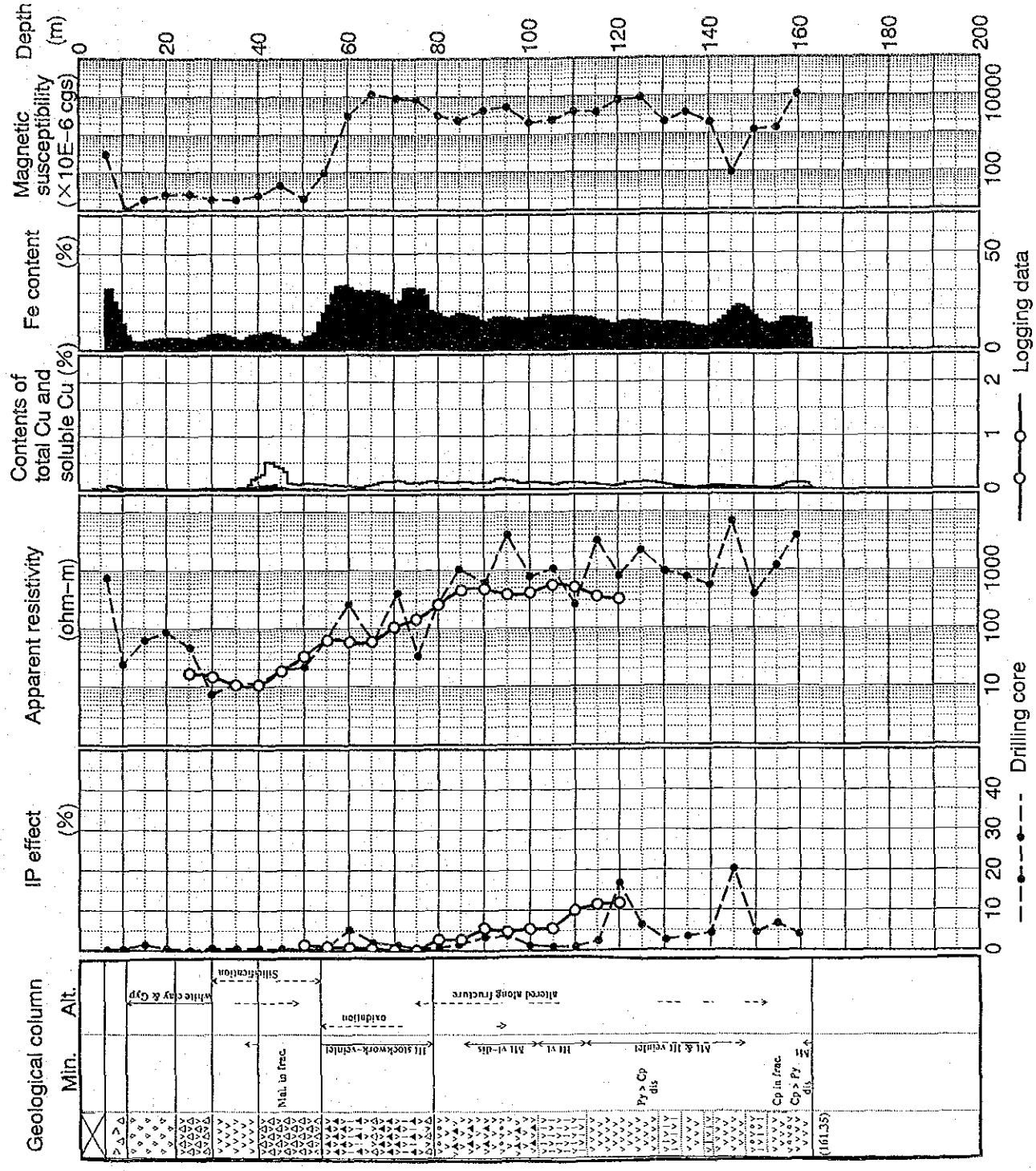

Fig. II-4- 6 Synthetic column for MJCC- 6

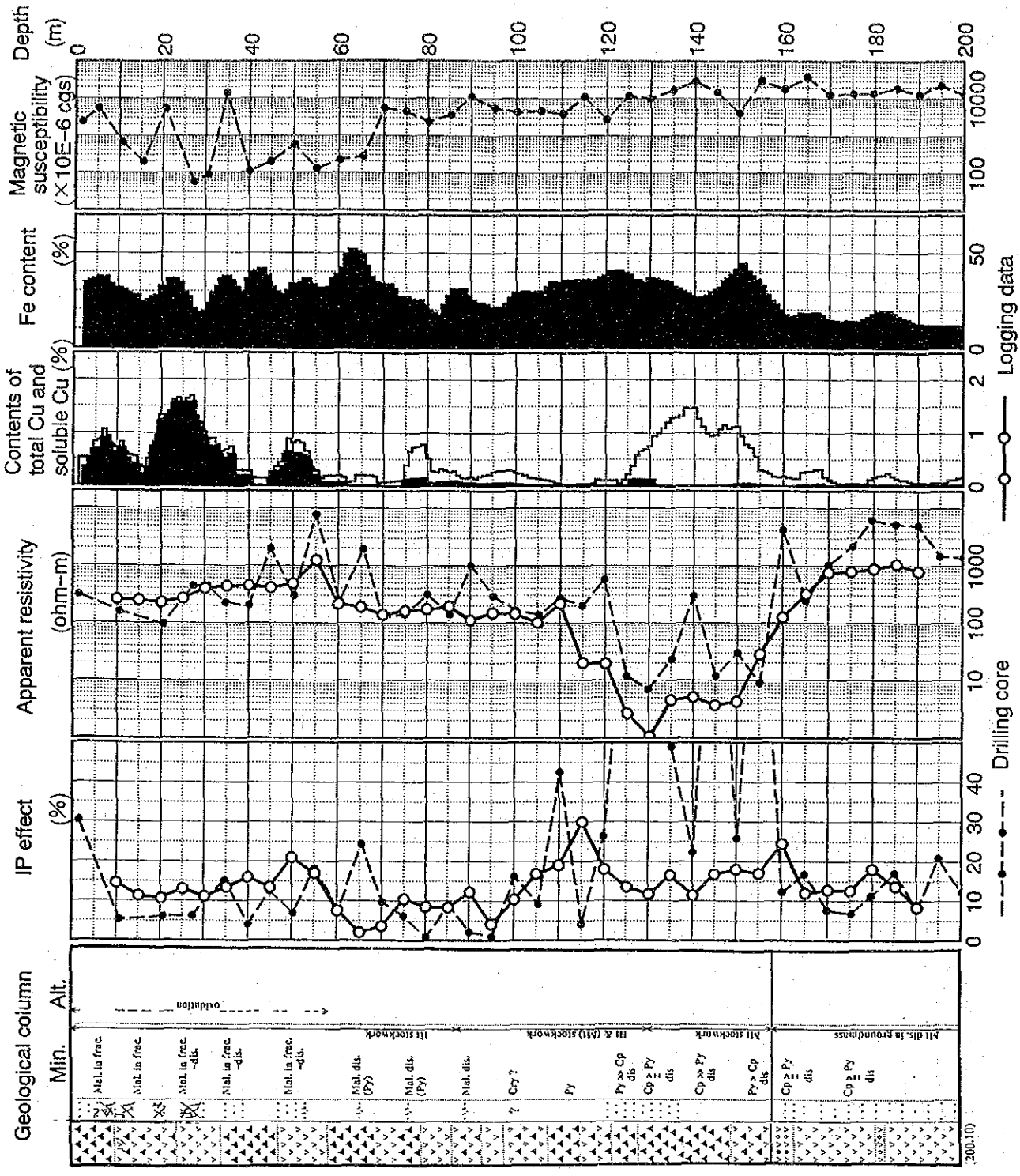

Fig. II-4- 7 Synthetic column for MJCC- 7

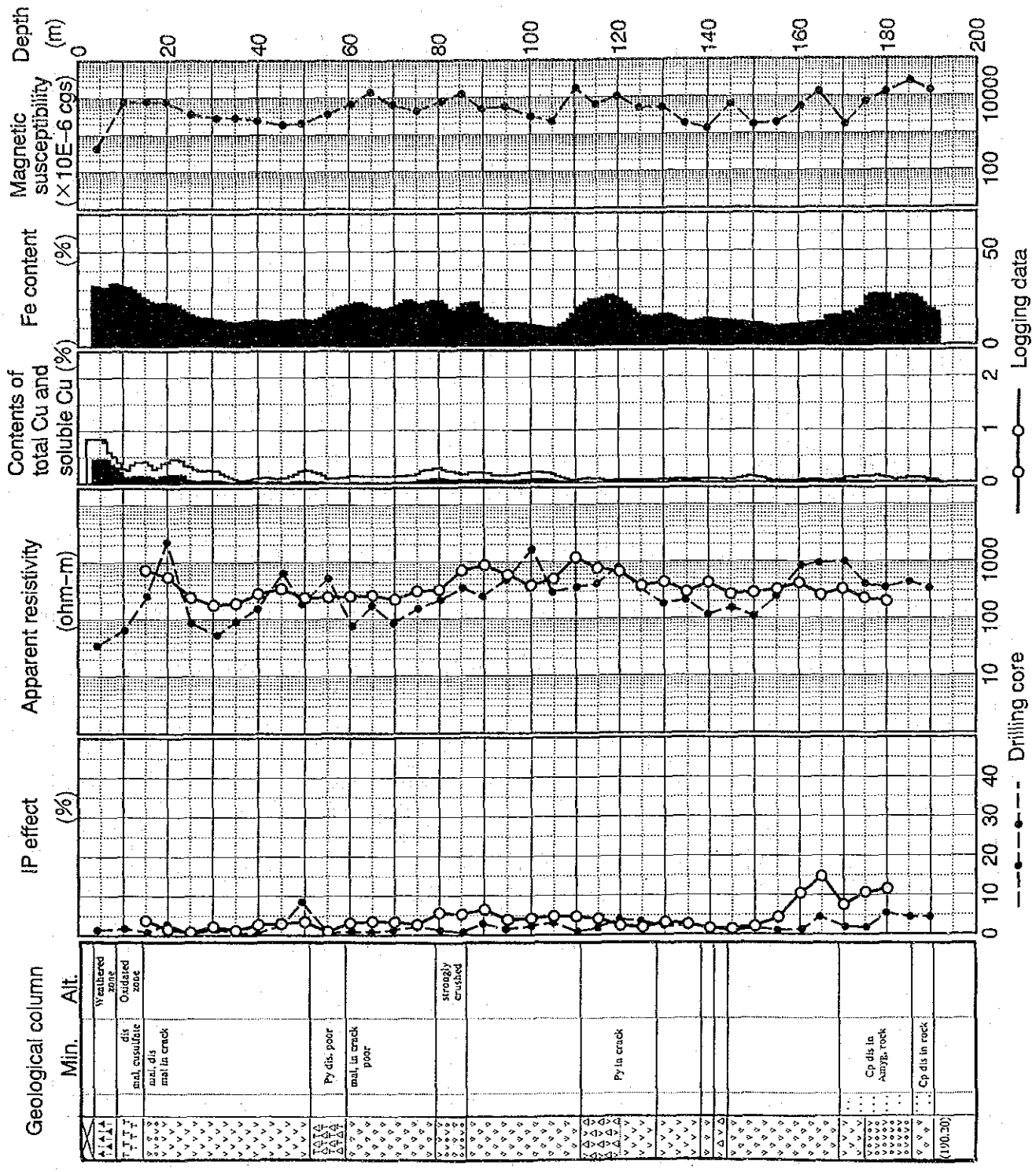

Fig. Ⅱ-4- 8 Synthetic column for MJCC- 8

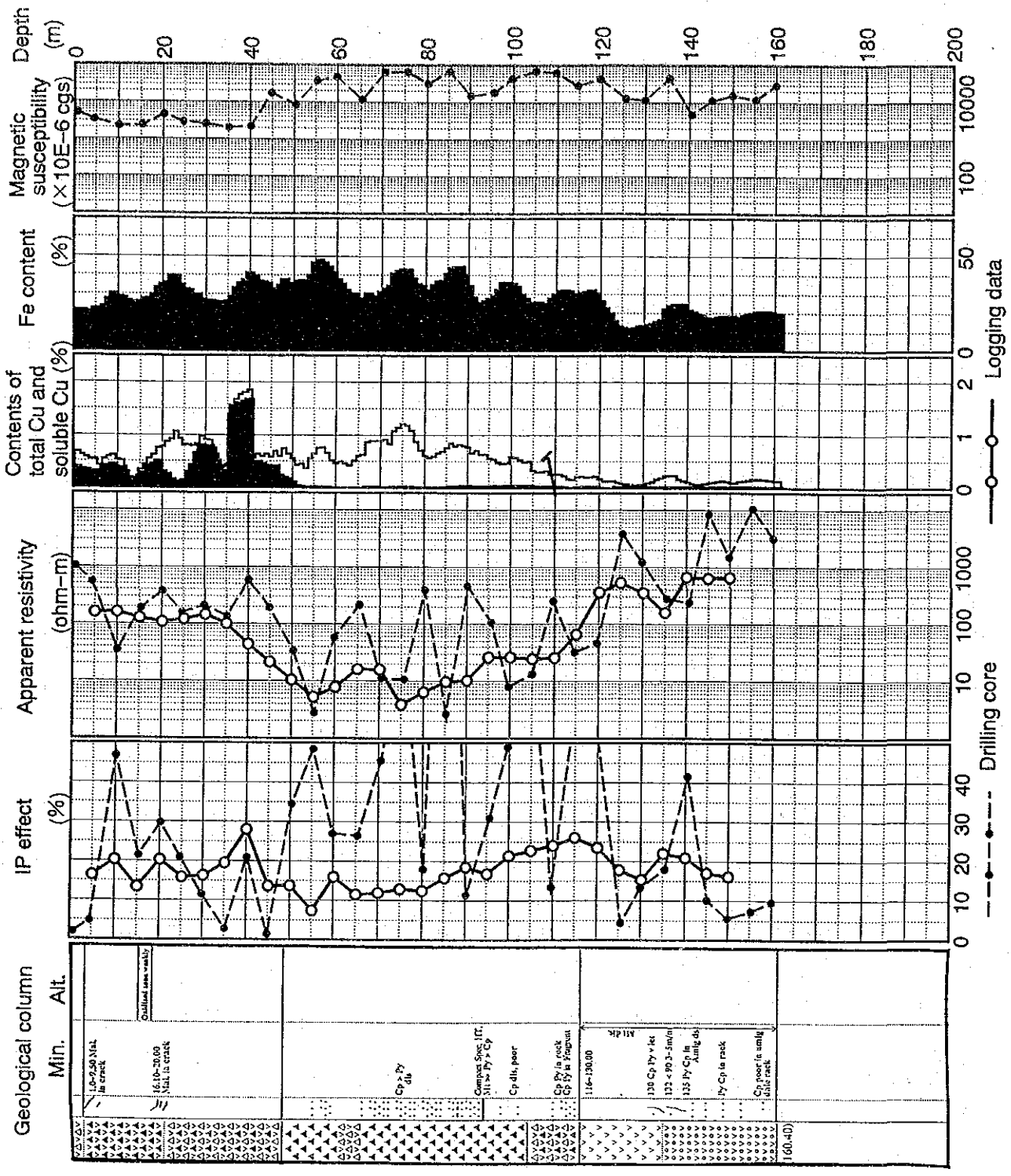

Fig. II-4- 9 Synthetic column for MJCC-10

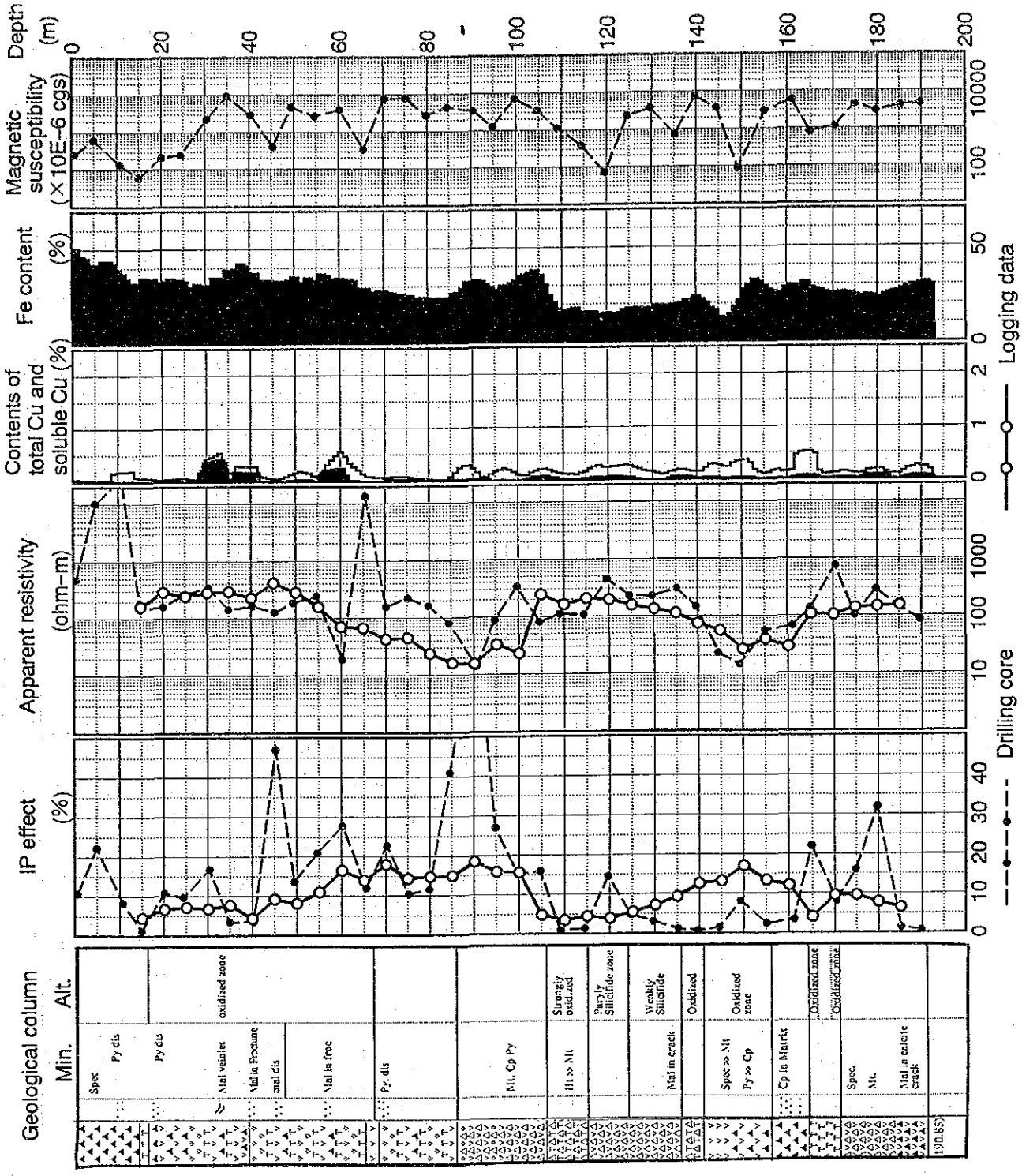

Fig. II-4-10 Synthetic column for MJCC-11

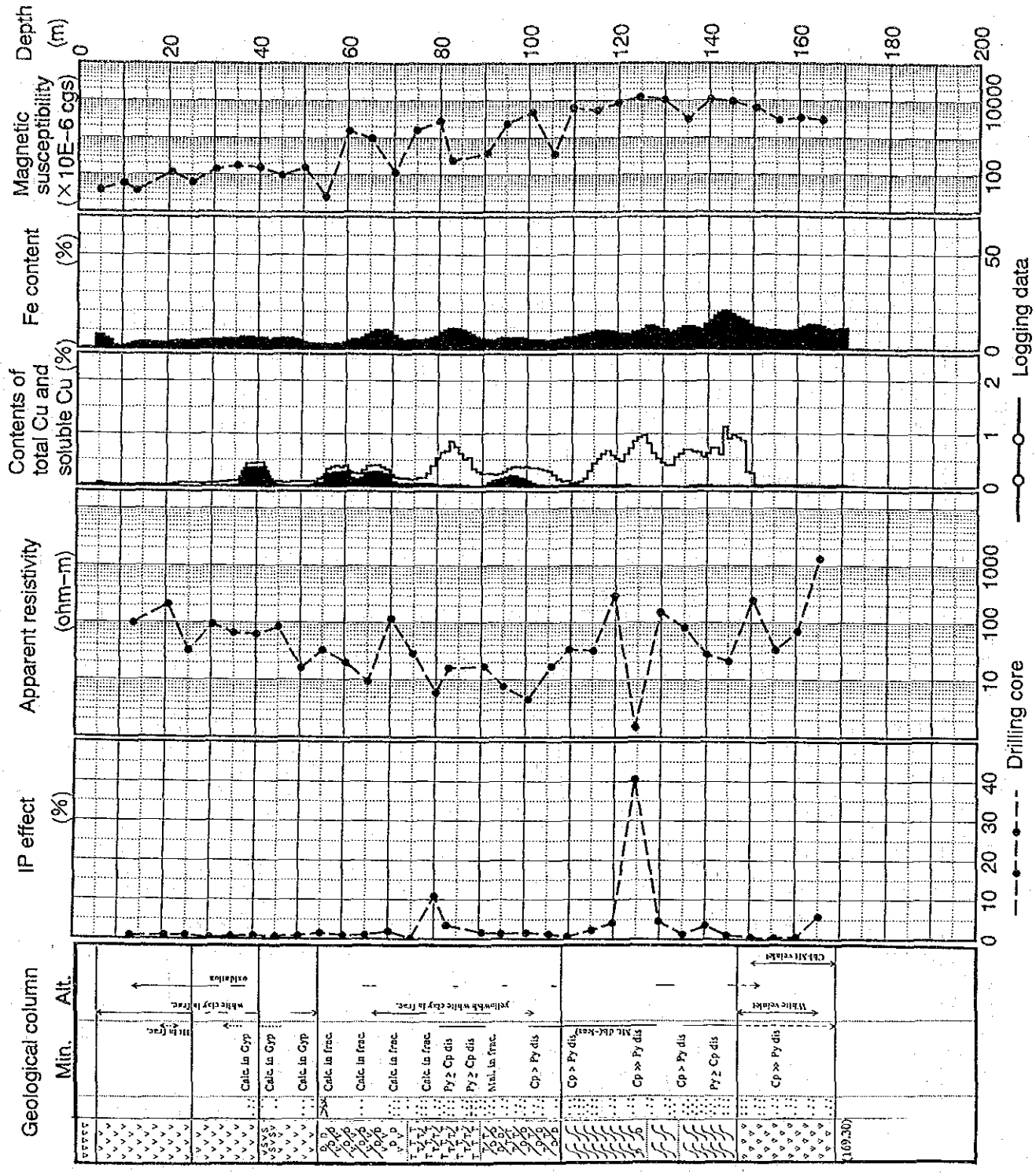

Fig. II-4-11 Synthetic column for MJCC-12

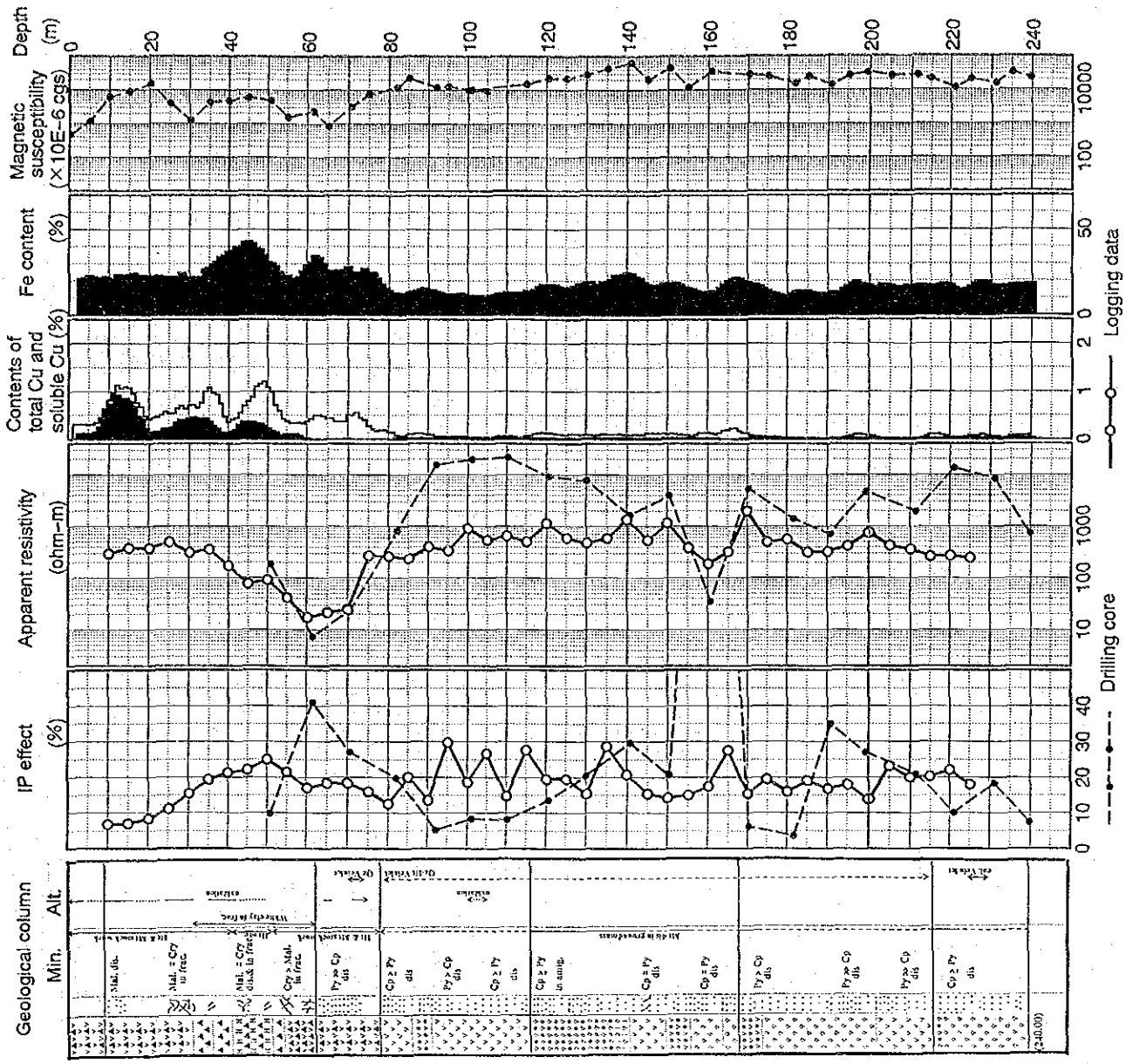

Fig. II-4-12 Synthetic column for MJCC-13

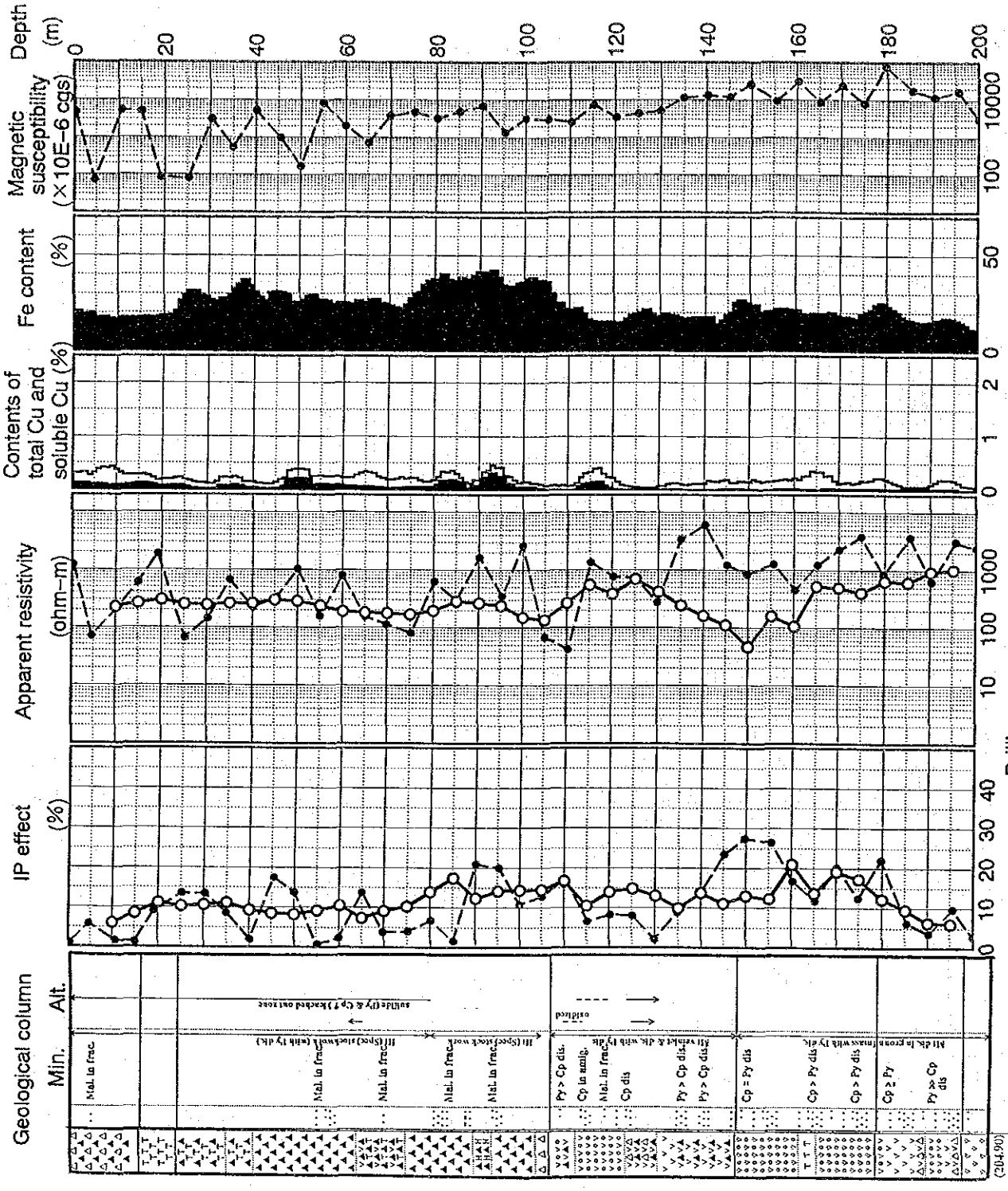

Fig. II-4-13 Synthetic column for MJCC-14

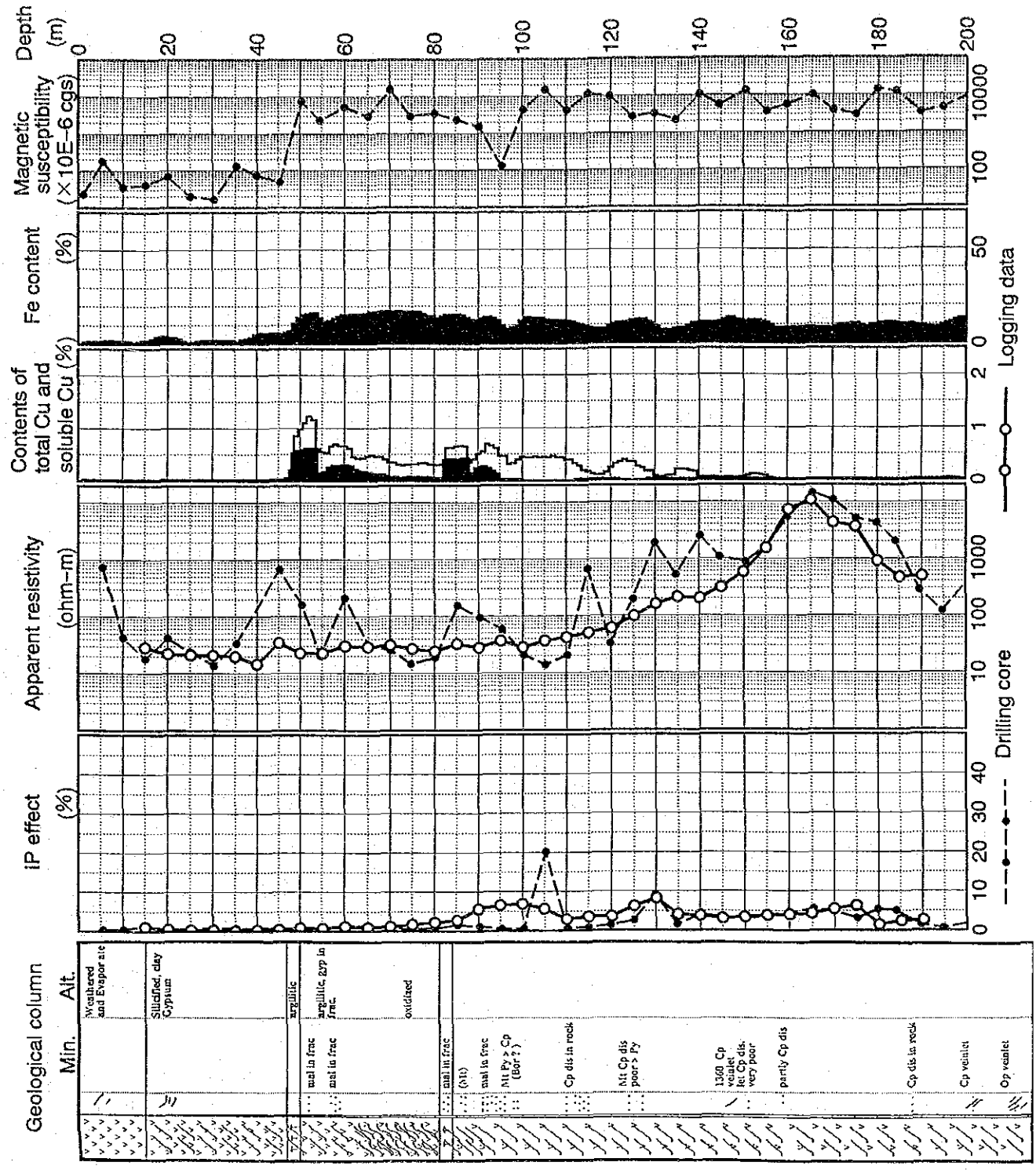

Fig. II-4-14 Synthetic column for MJCC-16

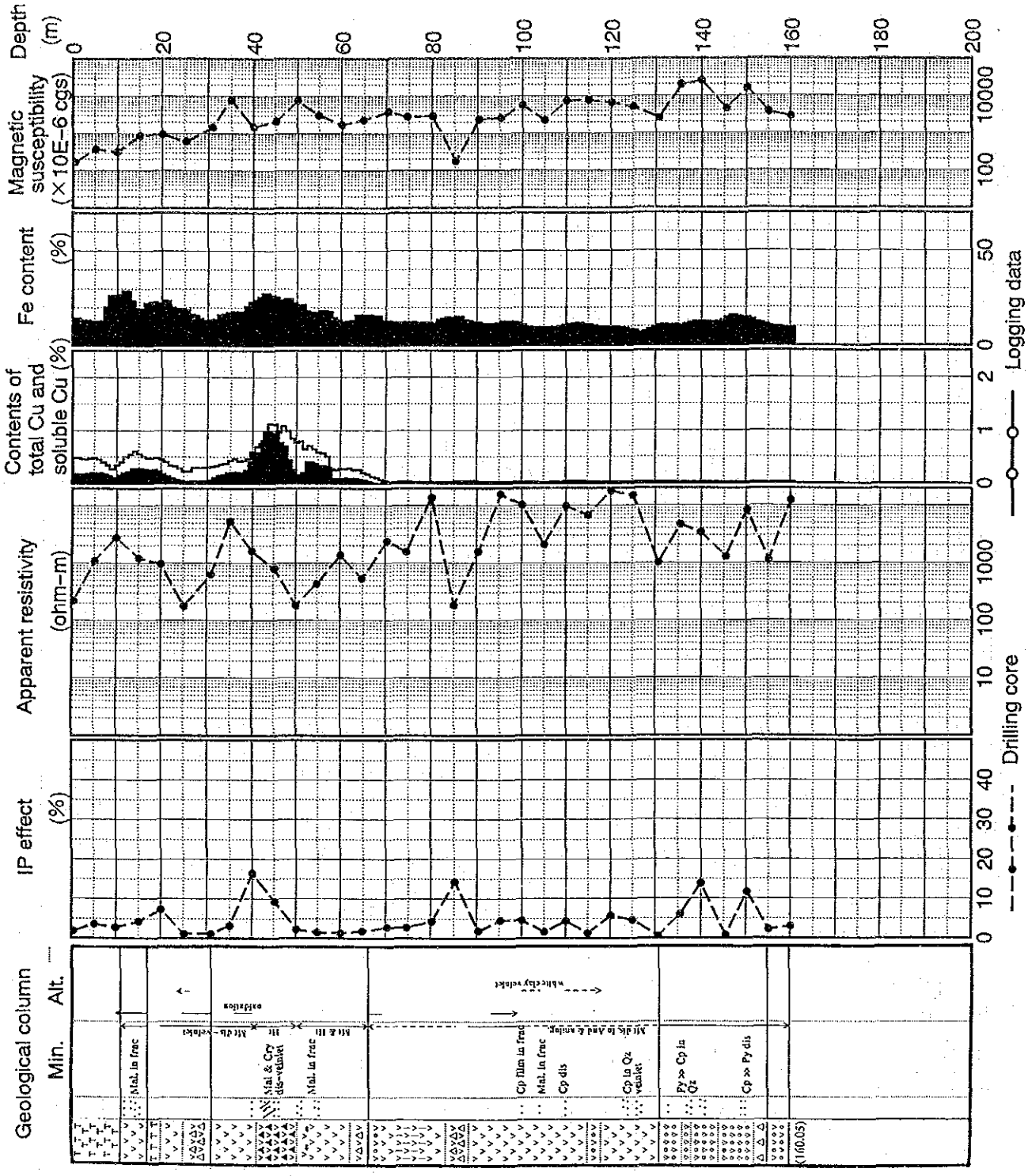

Fig. II-4-15 Synthetic column for MJCC-17

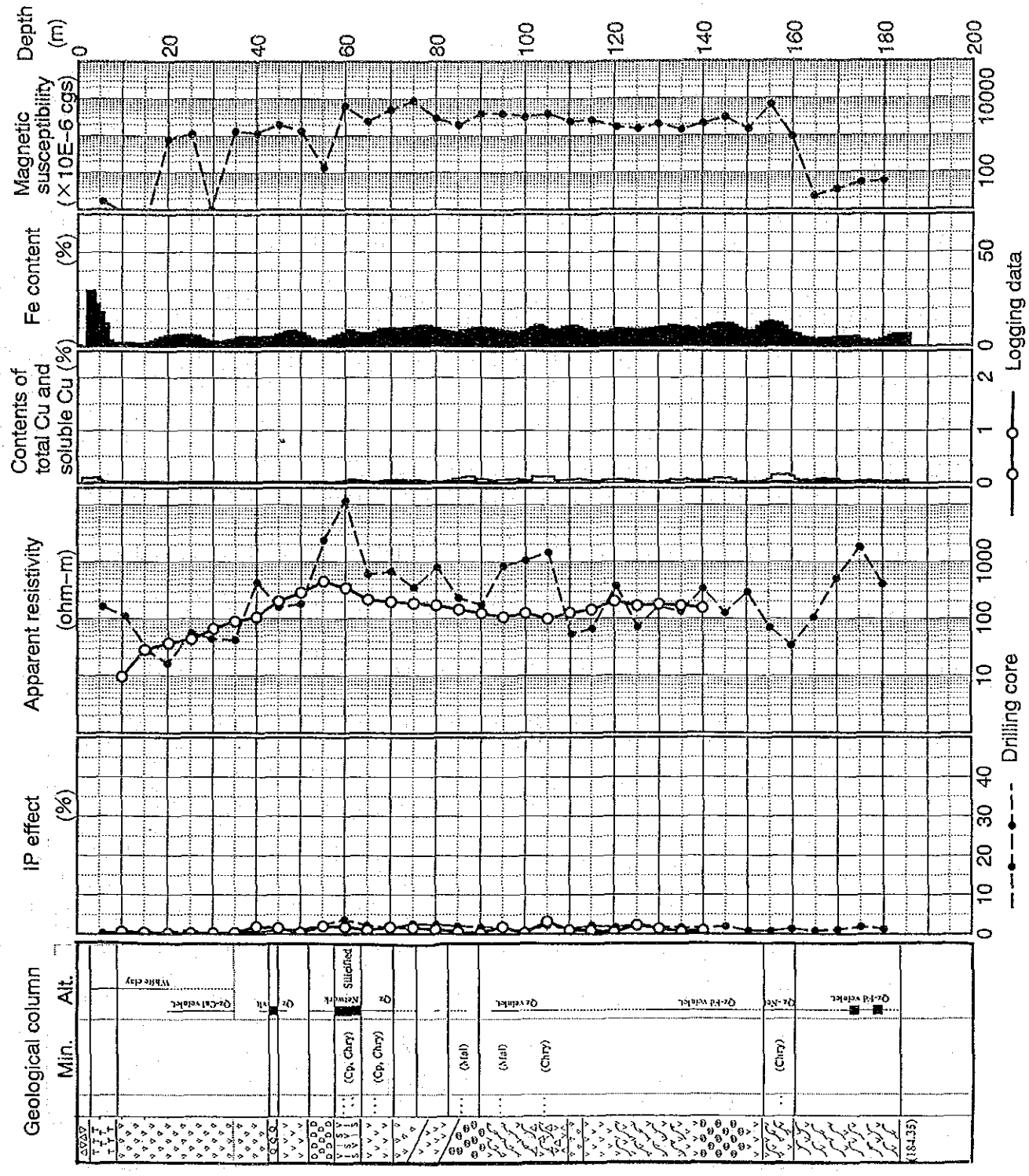

Fig. II-4-16 Synthetic column for MJCC-18

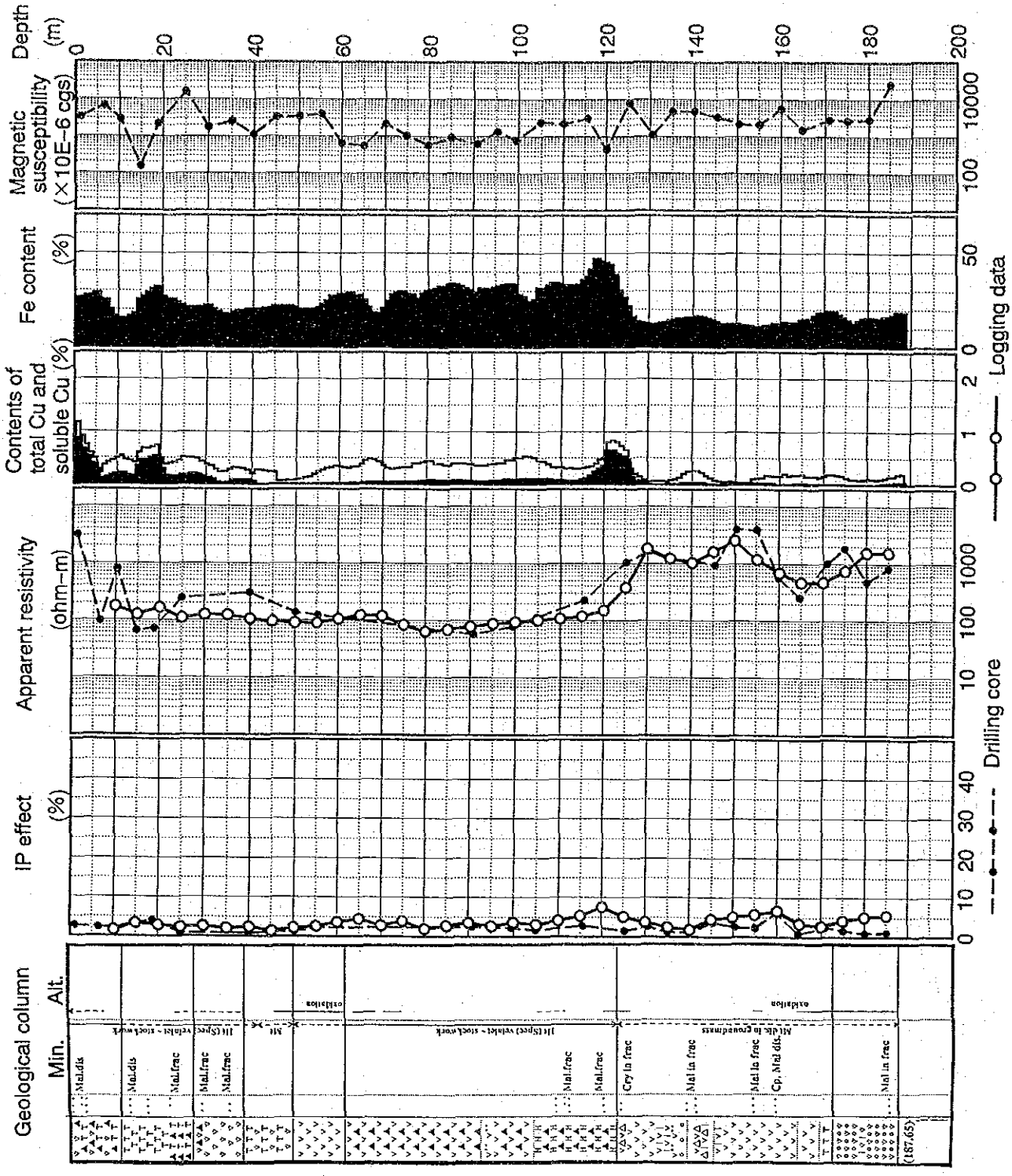

Fig. Ⅱ-4-17 Synthetic column for MJCC-20

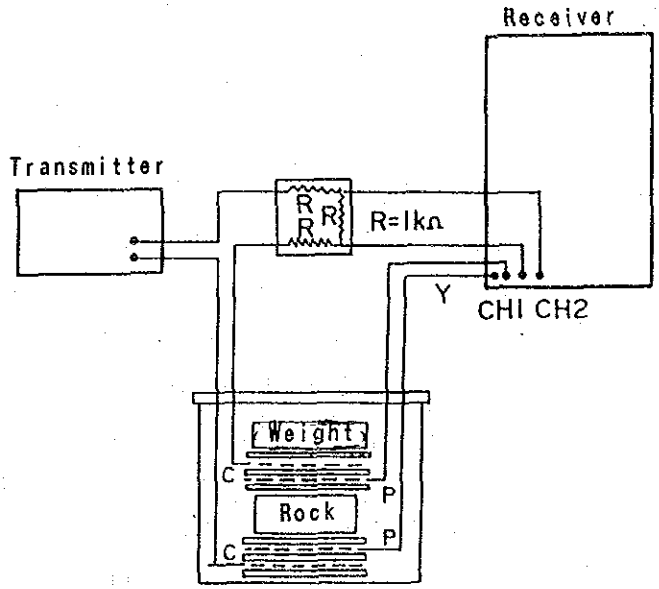

Fig. II-4-18 General idea of measurement for core sample

4-2-2 Equipment for measurement

The equipment used for measurement are as shown in the following Table II-4-4:

Table II-4-4 Equipment/Materials for Material Measurement

Name of Equipment	Type of Equipment	Function/Performance
IP Transmitter for sample measurement	MODEL CH-8002A (Mfd. by Chiba Denshi K.K.)	Frequency Transmitted: 3.0, 0.3Hz, TD (2Sec) +/-DC Output Current : 1, 2, 5, 10, 20, 50, 100, 500, 1000 μ A Power Supply : 006P(9V) x 4
IP Receiver	(Frequency-domain) MODEL CH-8104R (Mfd. by Chiba Denshi K.K.)	Frequency Received : 3.0, 1.0, 0.3, 0.1Hz Input Level : 0.1mV to 10.0V Power Supply : 006P (9V) x 2
	(Time-domain) MK III (Mfd. by Huntec Co., Canada)	Frequency Received : 2Sec Input Level : 30 μ V to 10V Power Supply : 12V battery
Magnetic Susceptibility Meter	MODEL 3101A (Manufactured by Bison Co.)	Measurement Range : 0 to 100,000 $^{-6}$ cgs Power Supply : TR-234R (5.4V) x 2 Outer Coils (accessories): Type 3110-5 (ϕ 51mm) Type 3110-6 (ϕ 64mm)

4-2-3 Measurement results

According to the survey specifications, the number of items for measurement is designated as 458 for magnetic susceptibility. However, since it was necessary to study the relationship between the measurement results with the values obtained by chemical analysis in order to examine in detail the cause for abnormal IP, we decided to perform measurement of both magnetic susceptibility and IP for the core samples taken at intervals of 5m.

In accordance with Integrated Histogram for each drill hole (Figs. II-4-6 through II-4-17), IP logging data for individual drill holes and drill core measurement (Table II-4-3), the results of our drill core measurement are as follows:

(MJCC-6): Fig. II-4-6

While the average magnetic susceptibility for the depth from 0 to 60m is low indicating around 20(x 10^{-6}cgs emu - hereinafter to be omitted), the data for the depth of 60m and deeper are very high indicating 1,000 to 10,000. This characteristic variety is in a good conformity with the variety in iron content. IP and resistivity values of core are virtually the same as IP logging results.

(MJCC-7): Fig. II-4-7

While the average magnetic susceptibility is 3,000 for the depth from 0 to 100m, the average magnetic susceptibility for 100m and deeper is higher indicating 14,700. However, this does not correspond with the variety of iron content. IP value of drill core for the depth from 120 to 160m is high indicating 50% in correspondence with an ore-forming zone of the sulfide. Resistivity values are virtually in conformity with the logging data.

(MJCC-8): Fig. II-4-8

The magnetic susceptibility values of 2,000 to 10,000 has a little variety for the depth from 0m to the hole bottom, and it shows a tendency to interlock with iron content. The IP and resistivity values are in good conformity with the logging results.

(MJCC-10): Fig. II-4-9

While the average magnetic susceptibility for the depth from 0tothe hole bottom is approx. 24,000 which is the highest result in this study, that for the depth from 0 to 40m is around 2,000 which is rather low. The average IP of drill core for the depth from 0m to the hole bottom indicates 30% which is the highest result in this study. The relationship between high IP values and low resistivity is clearly seen accompanied by a good conformity with an ore-forming sulfide. In general, the swing of changes is far larger than that of the logging results.

(MJCC-11): Fig. II-4-10

The magnetic susceptibility values indicating from 100 to 1,000 is full of variety and the average is 2,900, IP values of drill core at two kinds of depth, 45m and 90m, are as high as around 50% and the swing of changes is larger than that of logging data.

(MJCC-12): Fig. II-4-11

Magnetic susceptibility shows a tendency to increase as the measurement depth increases, indicating around 100 for the depth from 0 to 50m, approx. 1,000 for the depth from 60 to 110m, and approx. 10,000 for the depth from 110 to 165m. IP values of drill core are low in general indicating 2 to 3%. However, for the depth of 125m both IP and resistivity values are high indicating 40% and 1.5 Ω·m respectively.

(MJCC-13): Fig. II-4-12

The average magnetic susceptibility is 23,000 which is the second highest value to that of MJCC-10. It has a tendency to show high values for the depth of 100m and deeper, but no correspondence with iron content is noticed. The average IP value of drill core is 25.3% which is also the second highest to that of MJCC-10. The resistivity values of drill core are also high indicating 10,000 Ω·m and over for the depth of 90 to 120m.

(MJCC-14): Fig. II-4-13

Magnetic susceptibility increases as the depth increases, indicating 10,000 and over for the depth of 140m and deeper, but no correspondence with iron content is noticed. Both IP and resistivity values of drill core have considerable variety in locality.

(MJCC-16): Fig. II-4-14

While the magnetic susceptibility values for the depth from 0 to 45m are low indicating around 100, those for the depth of 50m and deeper show a tendency of being high indicating 1,000 to 10,000. Both IP and resistivity values of drill core are in good correspondence with logging data.

(MJCC-17): Fig. II-4-15

The magnetic susceptibility shows a tendency to increase as the depth increases. IP data of drill core are mostly 5% and under but a higher IP value of 15% is noted in some locality. The average resistivity of drill core is approx. 2,000 Ω·m which is the highest in this study. The resistivity for the depth of 80m and deeper is especially high indicating 10,000 Ω·m.

(MJCC-18): Fig. II-4-16

While the magnetic susceptibility values for the depth both from 0 to 15m and from 165 to 180m are low indicating 100 and under, those for other depth are relatively high indicating 1,000 to 10,000. The average IP of drill core is 1.4% which is the lowest value in this survey.

(MJCC-20): Fig. II-4-17

Magnetic susceptibility values vary between 1,000 and 10,000 without any correspondence with iron content. Both IP and resistivity values of drill core coordinate with IP data; IP values are low indicating 5%, and resistivity values are around 100 Ω·m for the depth from 0 to 120m.

4-3 Analysis and study

With regard to the relationship between the IP logging results and abnormality in the surface IP, we studied the correspondence between these two factors by comparing the pattern of the plane distribution map based on the average drill core data of individual drill holes and the pattern of the

plane distribution map based on the results of simulated models of the surface IP anomaly. As to the correlation among the drill core data of individual drill holes as well as to the comparison among the measurement values of individual drill holes, we studied on basis of the correlation chart and the measurement values of typical reference samples. Further, in our reanalysis of abnormality in the surface IP, we performed two-dimensional section analysis of the finite element method on ENAMI's four traverselines P-2, 3, 4 and 7. using the IP data on the traverselines and the results of drill core measurement as control data. In our reanalysis of abnormal magnetism, we performed three dimensional analysis using the magnetic susceptibility values of drill core as control data.

4-3-1 Physical properties of typical reference samples

Since the ore-forming zone of sulfide in this area universally contains magnetite, specularite, hematite, etc., we collected typical reference samples each consisting of a single kind of mineral and performed the same observatory measurement. The results are as shown in Table II-4-5. From this data, the followings are pointed out:

(1) The resistivity value of chalcopyrite is the lowest of 3 Ω·m, and its magnetic susceptibility of 27 x 10cgs is also the lowest.

(2) IP values of hematite are the lowest indicating 2.3 to 3.5%.

(3) IP values of specularite is high indicating 47.3%, while its resistivity values vary between 198 and 6,533 Ω·m.

(4) The IP values of magnetite are high indicating 21.0 to 48.0%, while its resistivity values vary between 171 and 8,777 Ω·m. Its magnetic susceptibility values are exceedingly high indicating 9,566 to 31,332 x 10-6cgs.

The above three features of physical property enabled us to establish divisions of individual mineral. The results of our study on the drill core data of are as described below.

Table II-4-5 Results of measuring geophysical properties for standard samples

	IP effect	Apparent resistivity	Magnetic susceptibility
Chalcopyrite	36.0 %	3 Ω·m	27 ×10E-6cgs
Hematite -1	2.3	1,757	281
-2	3.5	13,615	272
Specularite-1	47.3	6,533	157
-2	9.6	198	-
Magnetite -1	22.0	8,777	23,624
-2	21.0	5,286	9,566
-3	48.0	171	313,332

4-3-2 Correlation between IP logging data and abnormality in the field IP survey

The distribution of the source of abnormal IP values as shown in Fig. II-4-1 have been estimated based on the results of model simulation enforced by ENAMI. The positional relationship between the source of abnormality and the trial drilling drill holes for IP logging is described below:

(1) The trial drilling drill holes situated in the substance with high IP and low resistivity values: MJCC-7, 10, 13, 14

(2) The trial drilling drill holes situated near the borders of the substance with high IP and low resistivity values: MJCC-8, 11, 16

(3) The trial drilling drill hole situated in the substance with high IP and high resistivity values: MJCC-20

(4) The trial drilling drill holes situated outside of the source of abnormal IP data: MJCC-6, 18

Based on the above positional relationship, the features of the distribution map obtained from the data of IP logging and materiality measurement (Table II-4-3) are as described below.

(IP distribution): Figs. II-4-19 and II-4-20

The IP distribution map shows similar tendencies for both logging and sample measurement data. The values are the highest in the vicinity of MJCC-10 and 13, and the range of high IP values extends to MJCC-7, 14 and 11. The development of such a zone with high IP values are in harmony with the existence of abnormal sources as estimated from the high values of the field IP survey, which proves that the simulation results have been correct.

(Resistivity distribution): Figs. II-4-21 and II-4-22

Owing to a wide-range difference among the resistivity values, we used logarithmic mean values in order to indicate the results. As far as the mean values are concerned, no definite zone of low resistivity is recognized related to the results of 100 to 200 Ω·m which are a little lower than those of vicinity. However, according to the integrated histogram, we note the existence of a zone with low resistivity values (logging data) of around 10 to 30 Ω·m in the trial drilling drill holes in correspondence with the source of abnormal IP data as per described below.

MJCC- 7: 1 to 5 Ω·m for the depth from 120 to 150m

MJCC-10: 4 to 20 Ω·m for the depth from 50 to 90m

MJCC-11: 15 to 30 Ω·m for the depth from 80 to 100m

MJCC-13: 20 to 30 Ω·m for the depth from 55 to 70m

The thickness of this low-resistivity zone is relatively thin indicating 15 to 40m. Since electric current concentratedly flows to the conductive layer caused by conductivity to earth, the surface IP seems to have detected the zone with high IP and low resistivity values.

(Metal conduction factor distribution): Figs. II-4-23, 24

Based on the high IP and low resistivity values of the source of abnormal IP data, we obtained

metal conduction factors for the individual IP logging and sample measurement data. The distribution map is as shown in Figs. II-4-3 and II-4-24. From these maps, we note that the results are in good conformity with the simulation model showing high IP and low resistivity values in its peak of metal conduction factor centering around MJCC-7, 10 and 13.

(Insoluble copper content distribution): Fig. II-4-25

The distribution of difference between the total copper content and soluble copper content, i.e. distribution of insoluble copper content, is shown in Fig. II-4-25. Because of the rare existence of insoluble copper oxide, most of insoluble copper content are almost similar to those of copper sulfide. From this map, it is pointed out that concentrated insoluble copper zone has been developed centering on MJCC-10 which overlaps with the portion having similar features of metal conduction factors and distribution of abnormally high IP values.

(Total-iron content distribution): Fig. II-4-26

The total iron content distribution is shown in Fig. II-4-26. A remarkable iron-enrichment behavior is noted in this district, and the universally existing magnetite and specularite may have given influence on IP as described below.

According to this chart, however, the trend of total iron content is NE-SW and no correspondence with IP and resistivity is recognized.

(Magnetic susceptibility): Fig. II-4-27

Magnetic susceptibility is shown in Fig. II-4-27. Since the scale of magnetic susceptibility mainly represents the magnetite content, we note from this chart that magnetite has been enriched centering around MJCC-10 and 13. As stated above, IP distribution shows the similar tendency as that of insoluble copper content distribution, it can be pointed out that insoluble copper and magnetite have been enriched centering on MJCC-10 and 13, by which abnormality in the IP data have been affected.

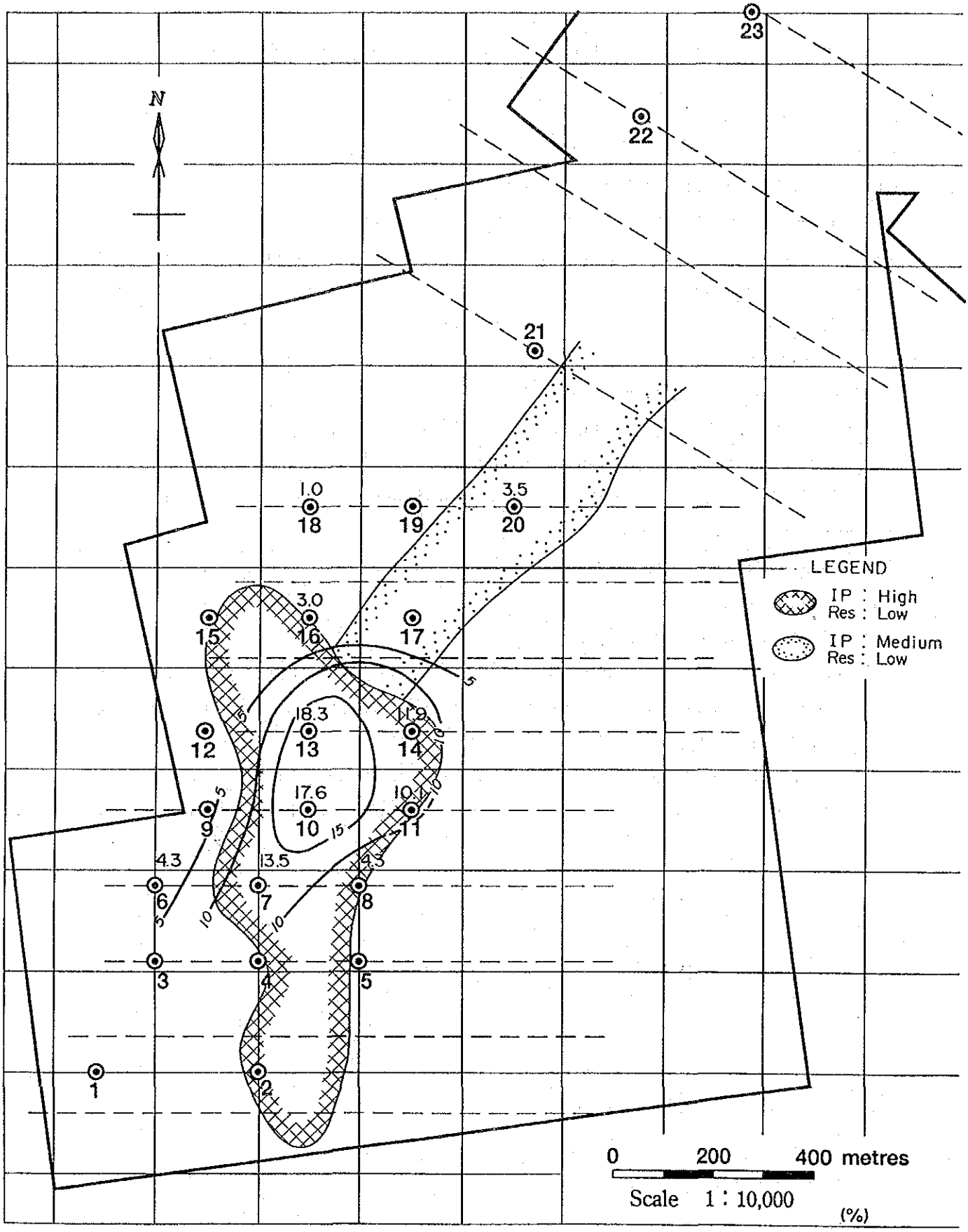

Fig. II-4-19 Distribution of IP intencity (logging)

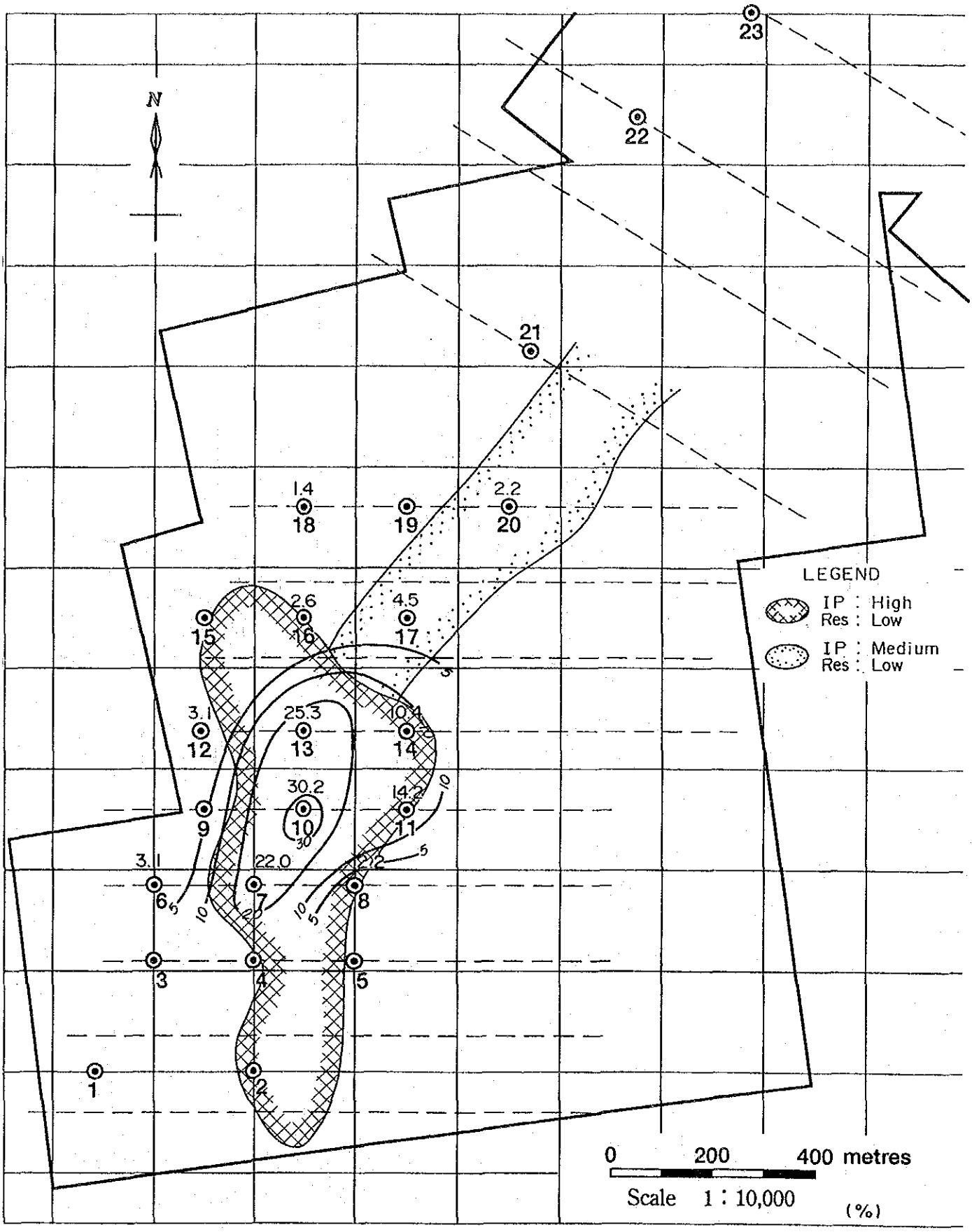

Fig. II-4-20 Distribution of IP intencity (core sample)

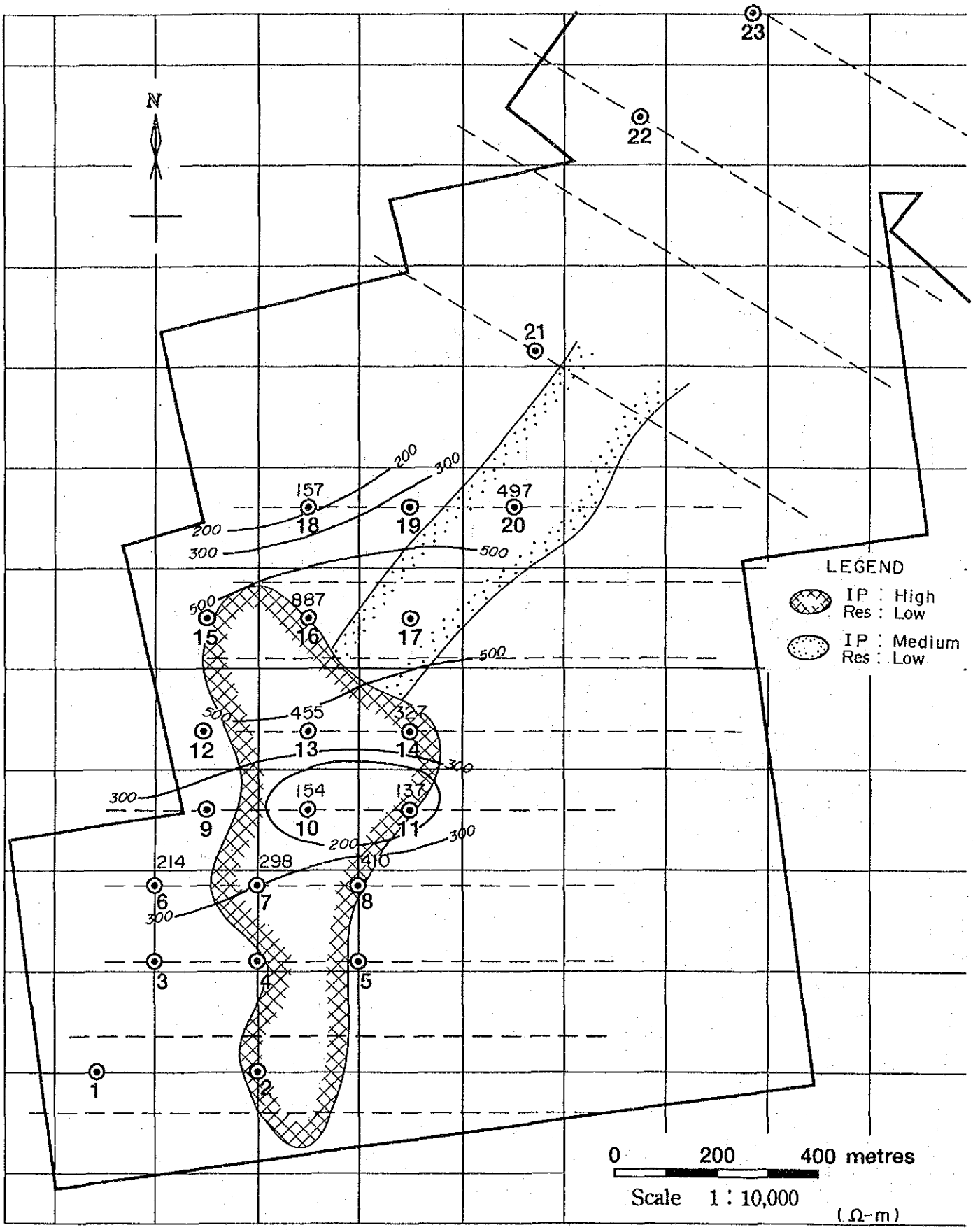

Fig. II-4-21 Distribution of resistivity value (logging)

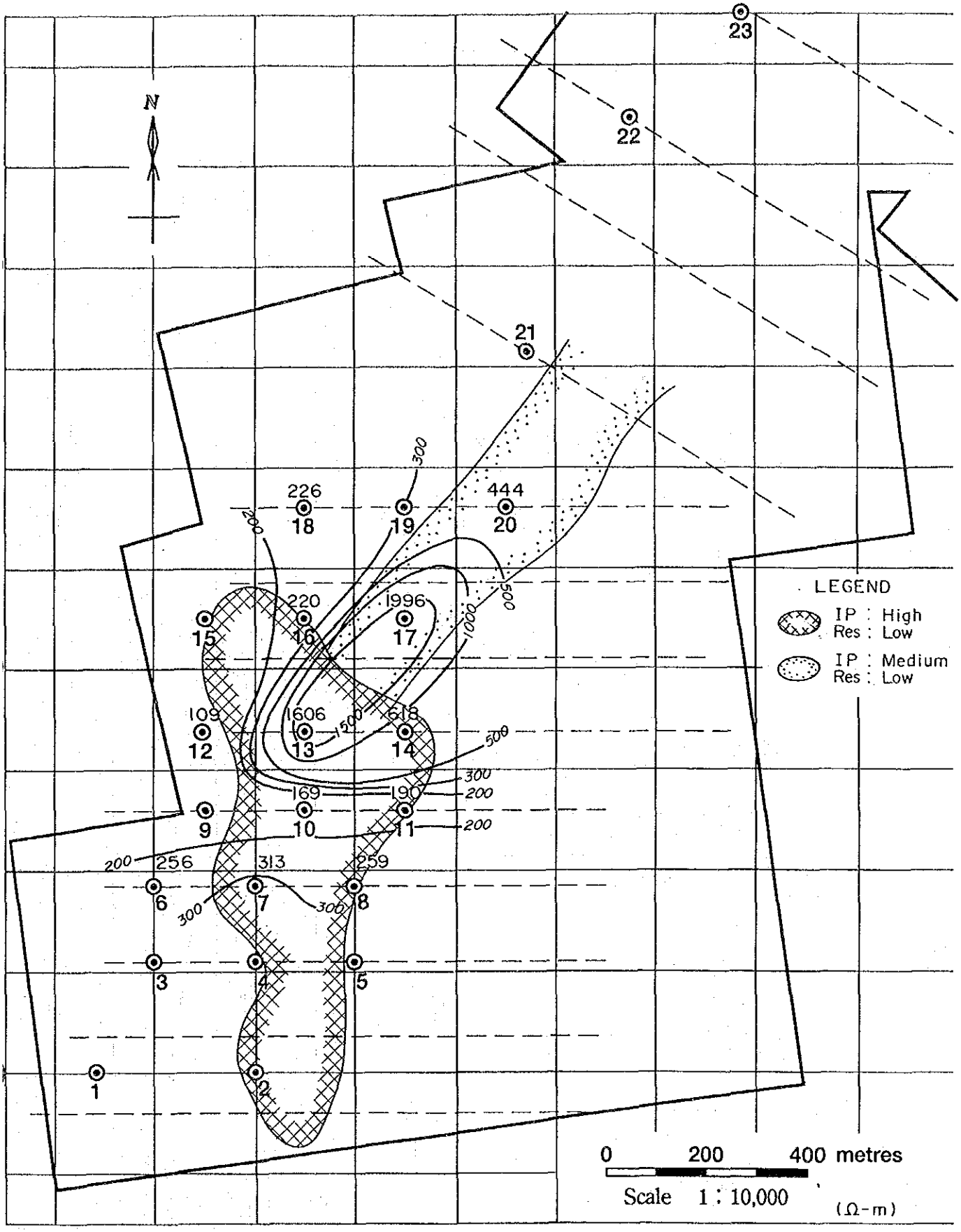

Fig. II-4-22 Distribution of resistivity value (core sample)

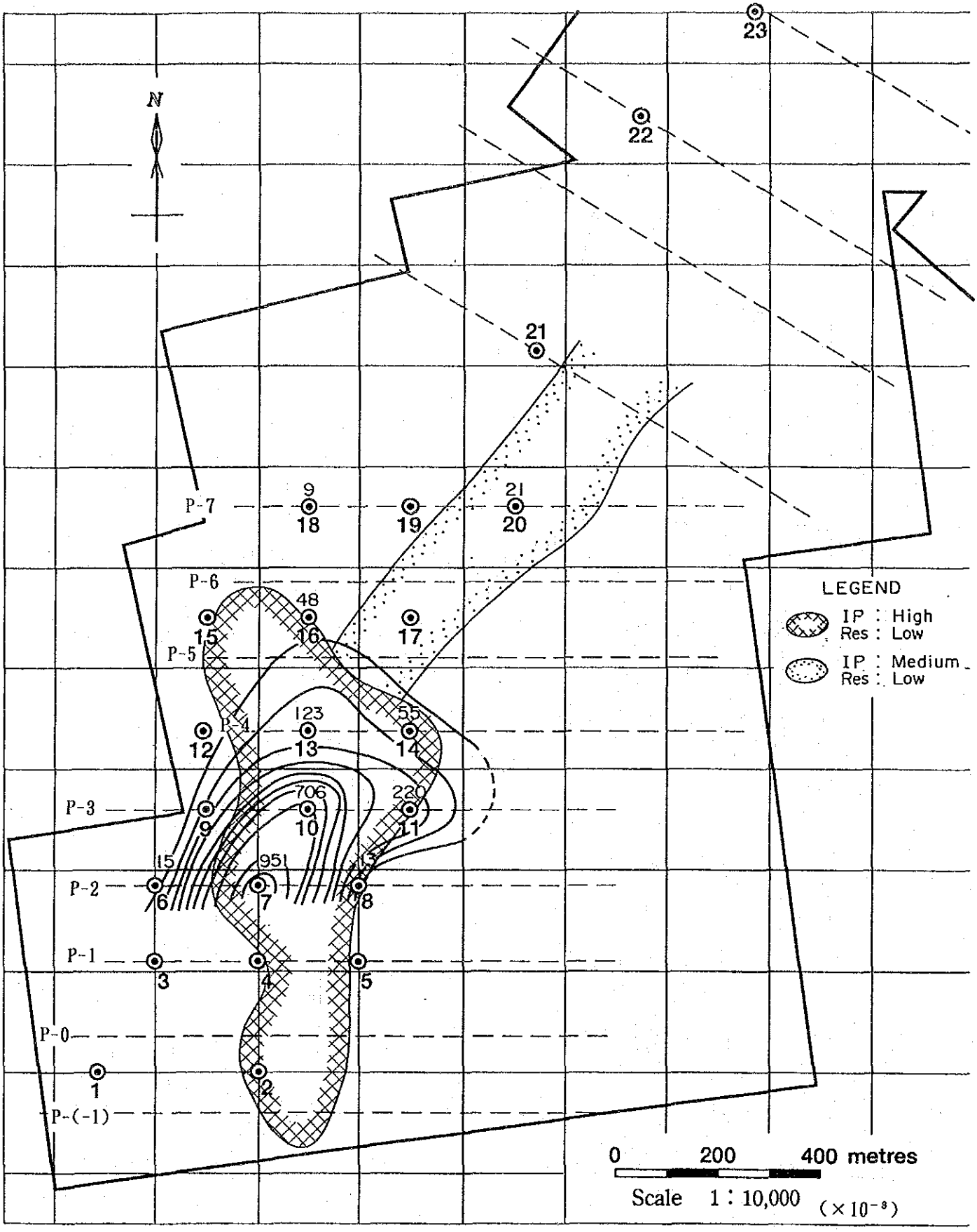

Fig. Ⅱ-4-23 Distribution of Metal facter (logging)

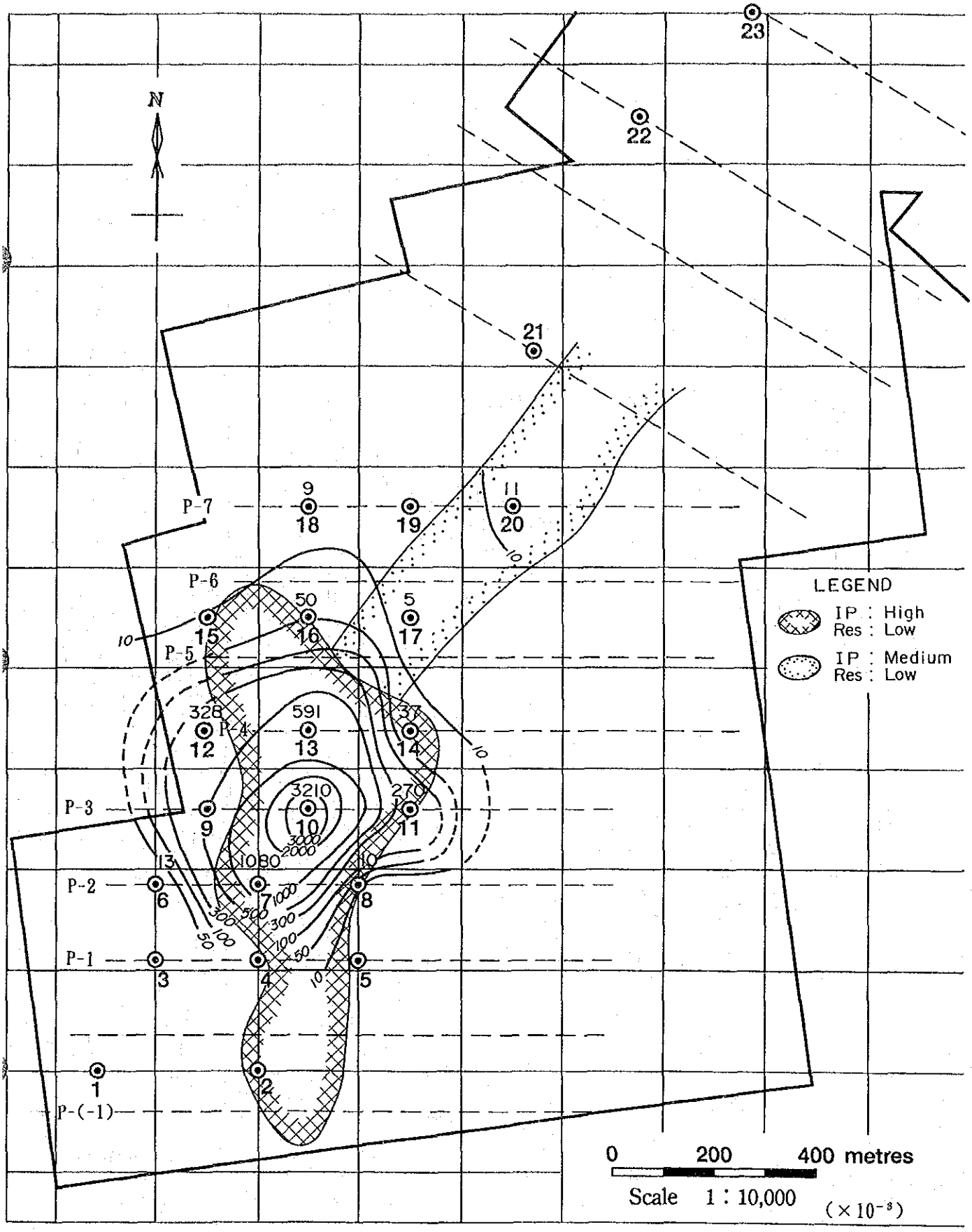

Fig. II-4-24 Distribution of Metal facter (core sample)

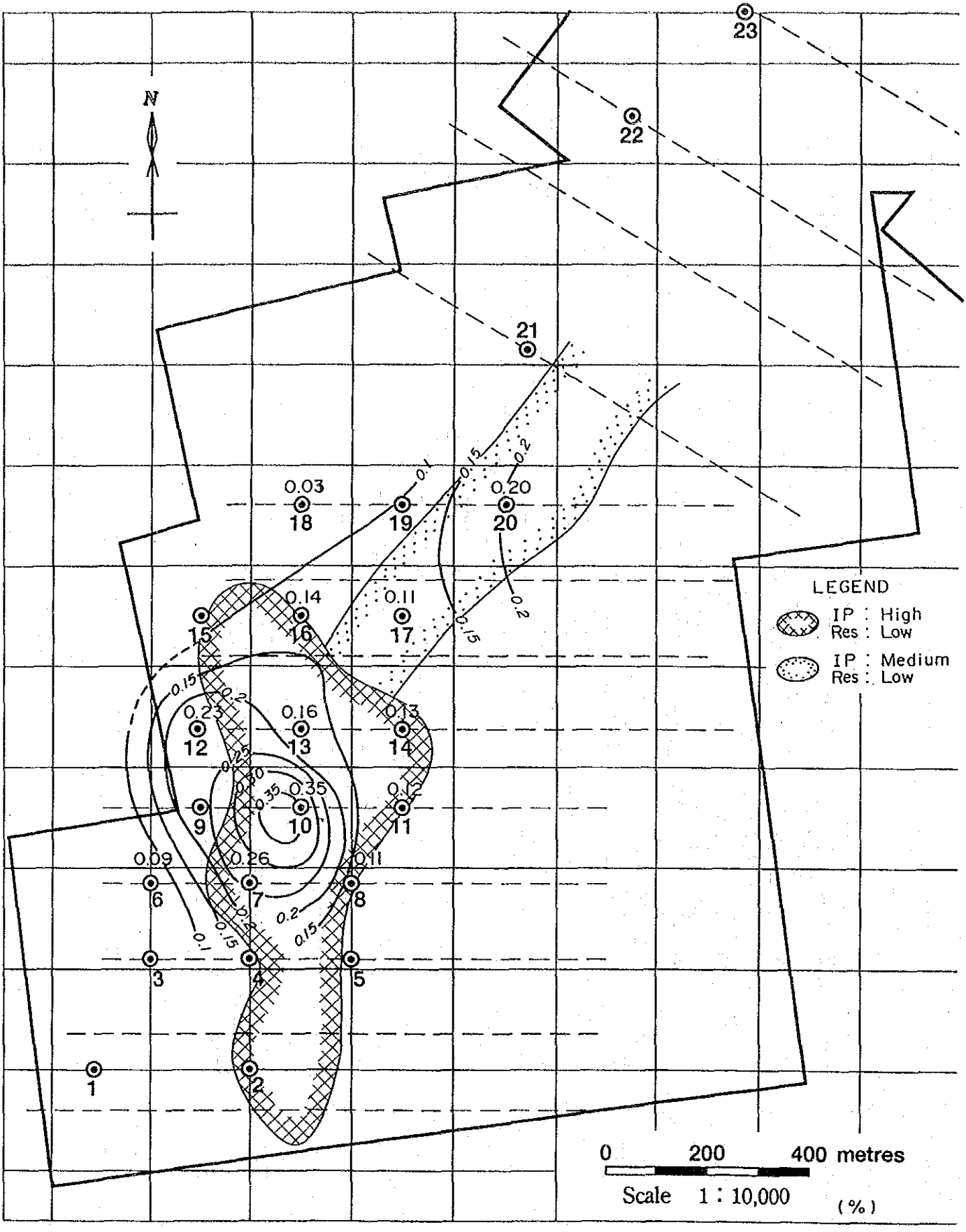

Fig. II-4-25 Distribution of insoluble Cu content

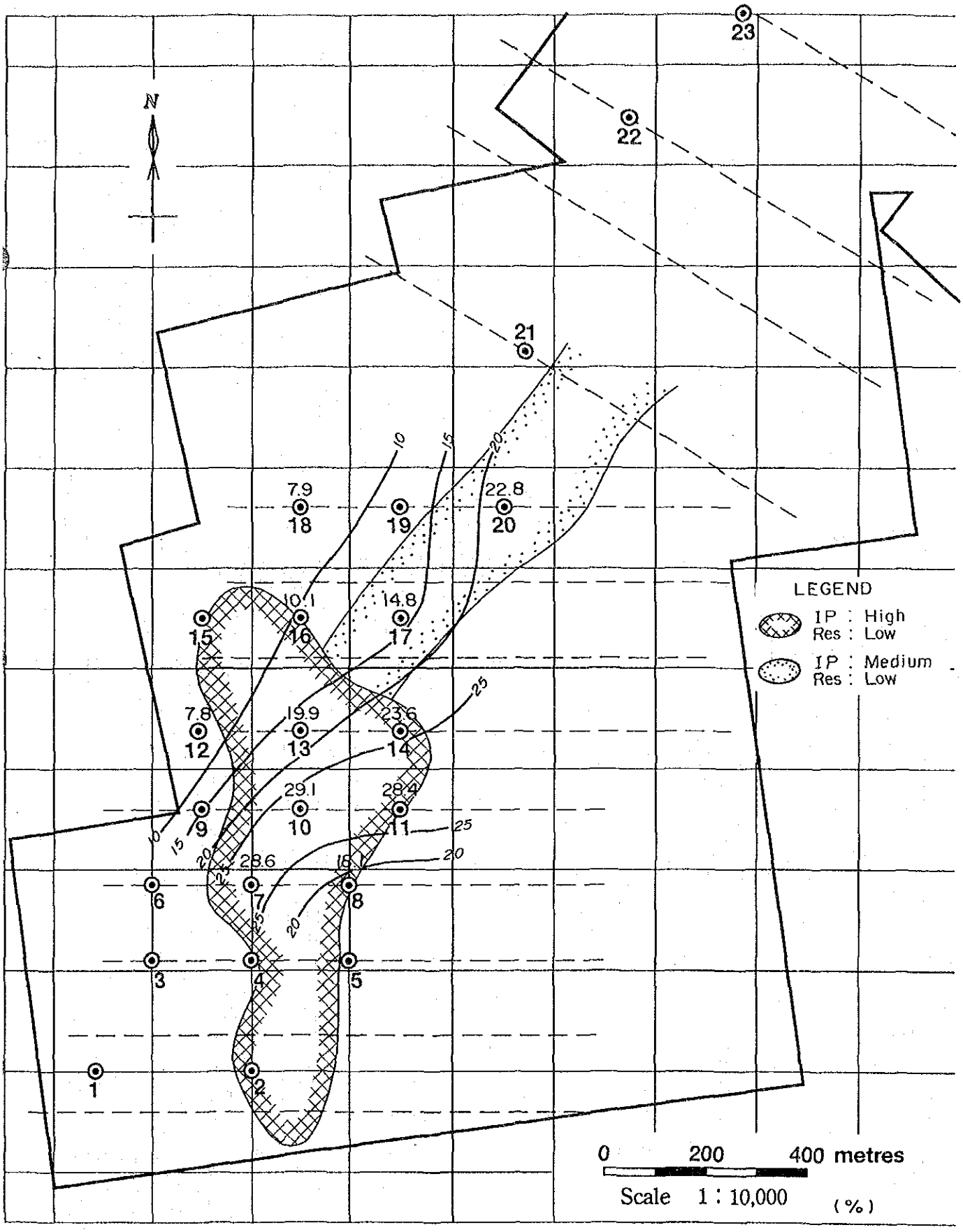

Fig. Ⅱ-4-26 Distribution of total Fe content

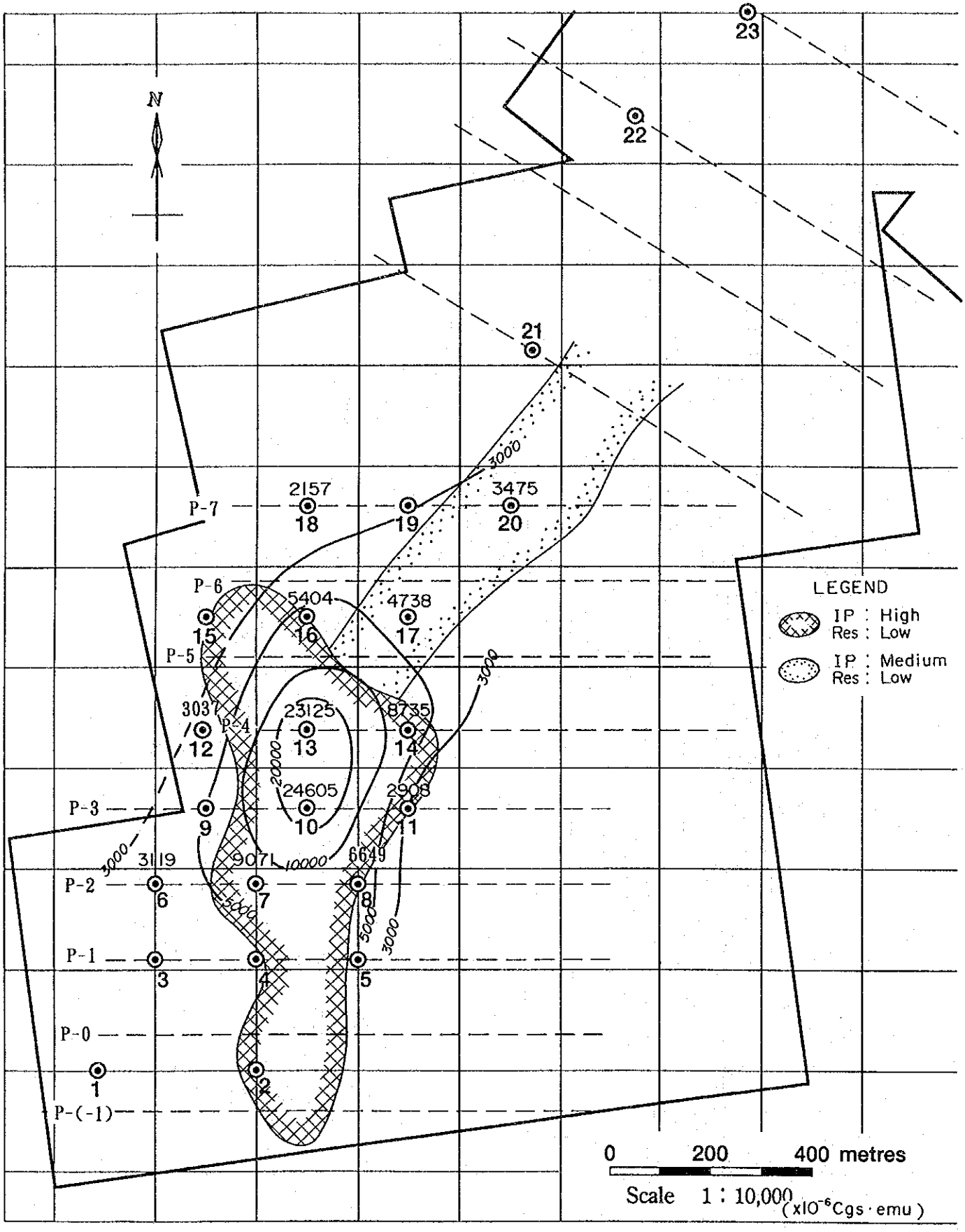

Fig. II-4-27 Distribution of Magnetic susceptibility

4-3-3 Results of the Re-Analysis of Surface IP Anomaly

IP anomaly, which was detected in field IP survey conducted by ENAMI, was reanalyzed by using IP well-logging data as control data. The method of analysis is a finite element method in 2.5 dimensions. The analytical targets consisted of four observations lines such as P-2 line (including MJCC-6, 7, 8), P-3 line (including MJCC-10, 11), P-4 line (including MJCC-12, 13, 14, and however by referring to data on the physical properties of cores for MJCC-12) and P-7 line (including MJCC-18, 20) in order of their locations from south. The analytical results of the observation lines are mentioned below.

(P-2 line): Fig. II-4-28

As for models explaining IP anomaly, the existence of two kinds of models such as a high IP with low resistivity model and a high IP with high resistivity model can be selected. The former corresponds to a chalcopyrite mineralization zone which was recognized to be located in hydrothermal breccia in MJCC-7 at a depth of 120 to 160m, and the zone is recognized to continue for 200 to 250m in the horizontal direction. The high IP with high resistivity model is distributed around the former high IP with low resistivity zone, and this model is assumed to correspond to a magnetite mineralization zone since it shows high resistivity.

(P-3 line): Fig. II-4-29

This is a survey line which traverses nearly the center of land surface IP anomaly from east to west. Its high IP with low resistivity model is assumed to be reflected by the continuity of a chalcopyrite mineralization zone which was recognized to be located in two places such as inside hydrothermal breccia in MJCC-10 at a depth of 50 to 100m and inside phenocryst andesite in MJCC-11 at a depth of 70 to 100m. This mineralization declines on its western side, and is assumed to horizontally continue for about 300m. A high IP with high resistivity model, which is assumed to be reflected by the existence of a magnetite mineralization zone in the same as P-2 survey line, is developed around this high IP with low resistivity model. Since the high IP zone on the eastern side of MJCC-11 was confirmed to be inferior by the calculation of the models, the prospecting potential is low.

(P-4 line): Fig. II-4-30

A model consisting of a chalcopyrite mineralization zone is assumed to continue in both eastern and western directions and was recognized to be located in hydrothermal breccia in MJCC-13 at a depth of 50 to 70m as a high IP with low resistivity anomaly source of land surface IP. This zone is assumed to continue for about 100m in each side of both directions. Based on the cross-sectional analysis of this model, a high IP with high resistivity zone is found to be developed above and below this high IP with low resistivity model and on the eastern side of the model, and a magnetite mineralization zone is assumed to be distributed in a wide area.

(P-7 line): Fig.II-4-31

According to the cross-sectional analysis of this area, a 30 to 50 Ω·m dike-shaped low resistivity

model is assumed to exist between MJCC-18 and MJCC-20, and this model can be compared with a fracture zone in the geological cross section. A dike-shaped weak IP with high resistivity model is assumed to exist on the eastern side of MJCC-20, and according to the geological cross section, this model corresponds to hydrothermal breccia accompanied by magnetite mineralization.

According to the combined results of the cross-sectional analyses mentioned above, a mineralization zone consisting of copper sulfide inside stockwork hydrothermal breccia is assumed to be developed in and around MJCC-7 as a high IP with low resistivity anomaly source of land surface IP, and the depth of its upper surface can be assumed to be controlled by the depth of the oxidation zone. This high IP with low resistivity zone exists together with a high IP with high resistivity zone, that is, a magnetite mineralization zone in its vicinity. Both zones are assumed to be closely related in the creation of ore deposits.

In making a comparison between the range of high IP with low resistivity zones, which was evaluated in the re-analysis, and the results of the past investigations, the range of the high IP with low resistivity zone along P-4 observation line can be mentioned to have decreased to 1/3 while MJCC-8 was placed outside the high IP with low resistivity zone and MJCC-11 was placed inside the zone (Fig.II-4-32).

According to the results of the cross-sectional analyses, the high IP with low resistivity zone regarded as the prospecting target is assumed to continue for a maximum of about 300m from east to west near MJCC-10. Since the continuity of the high IP with low resistivity zone can not be expected on the eastern side of Cerro Negro mountain ridge, the prospecting potential should be judged to be low.

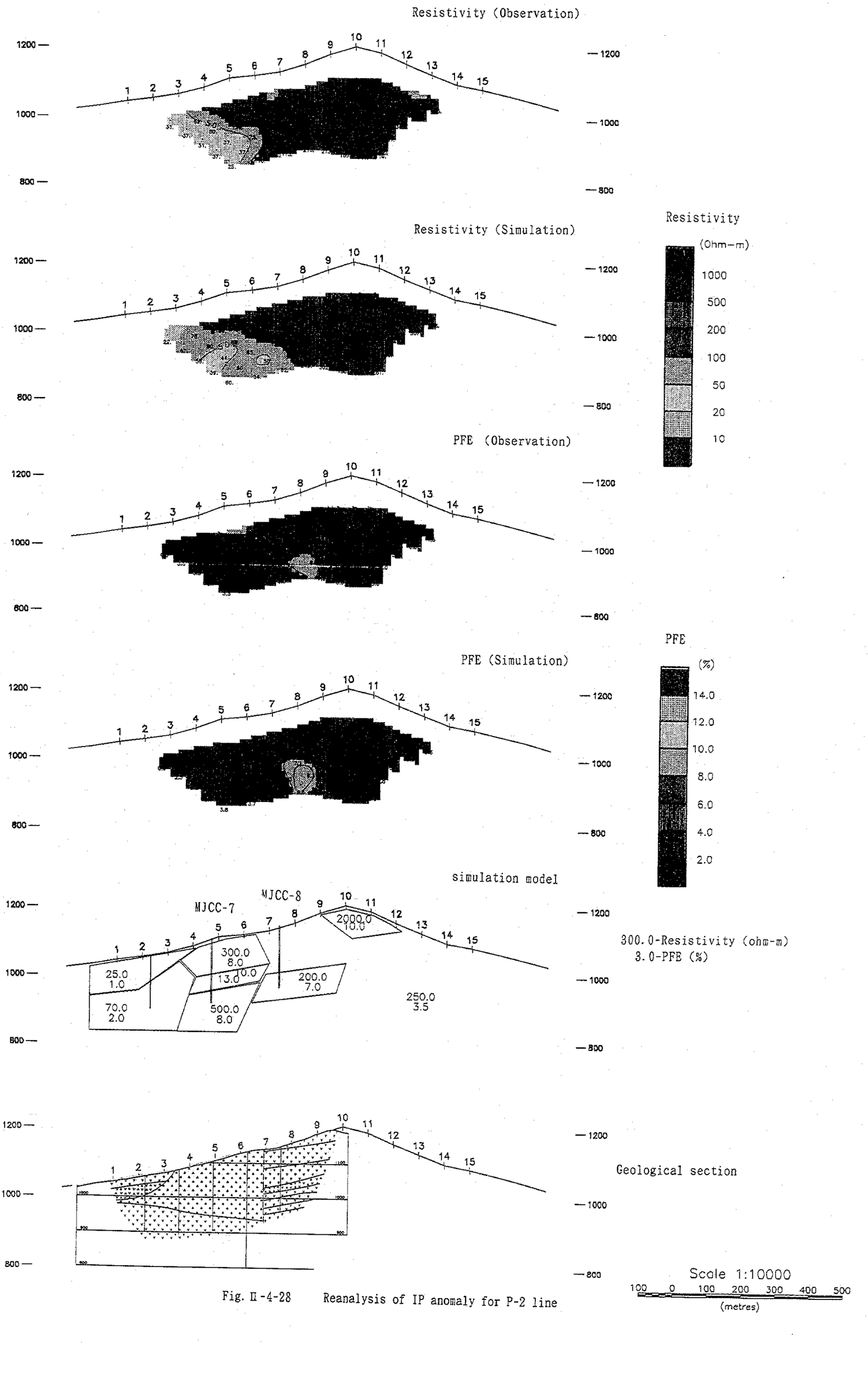

Fig. II-4-28 Reanalysis of IP anomaly for P-2 line

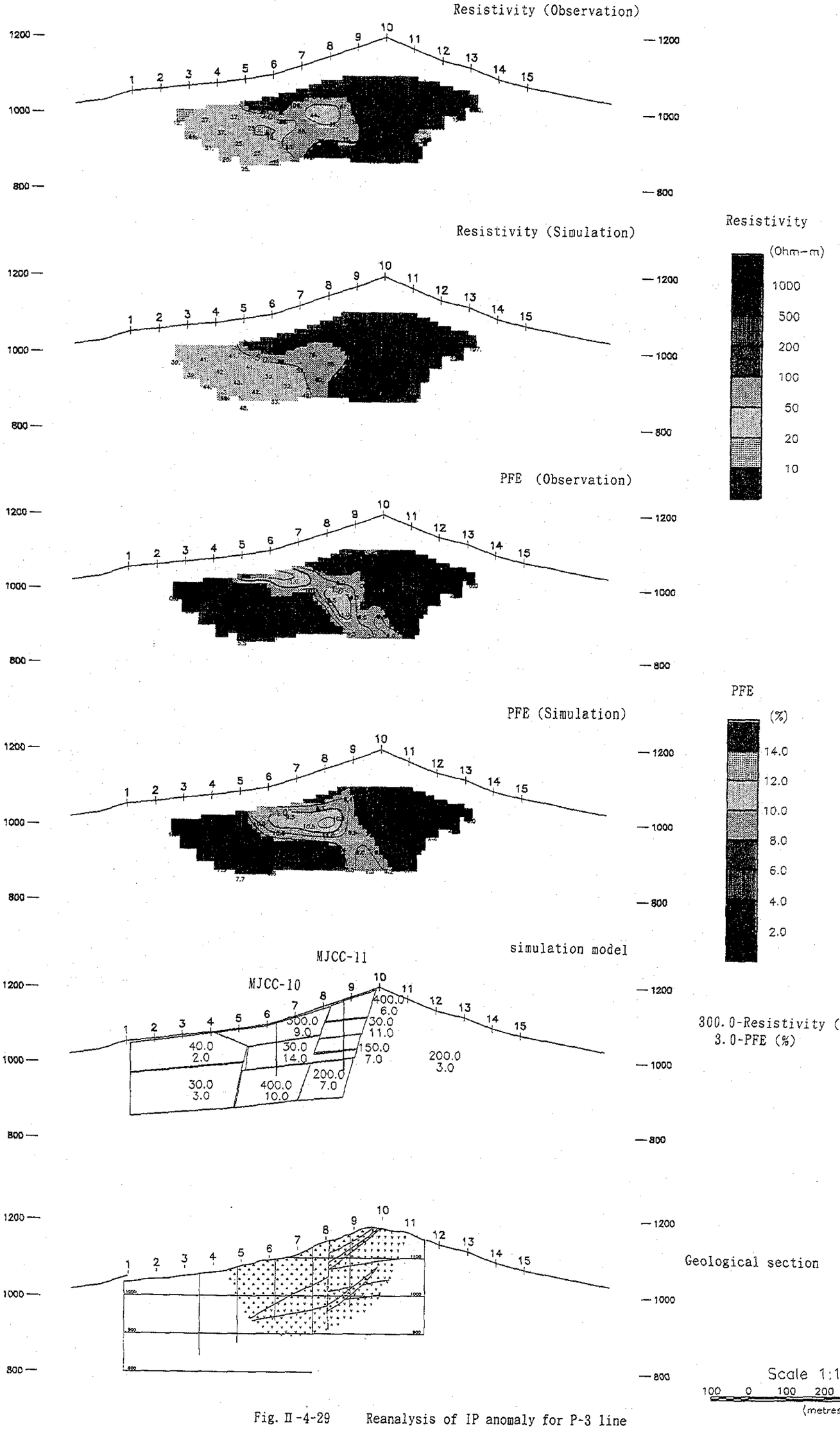

Fig. II-4-29 Reanalysis of IP anomaly for P-3 line

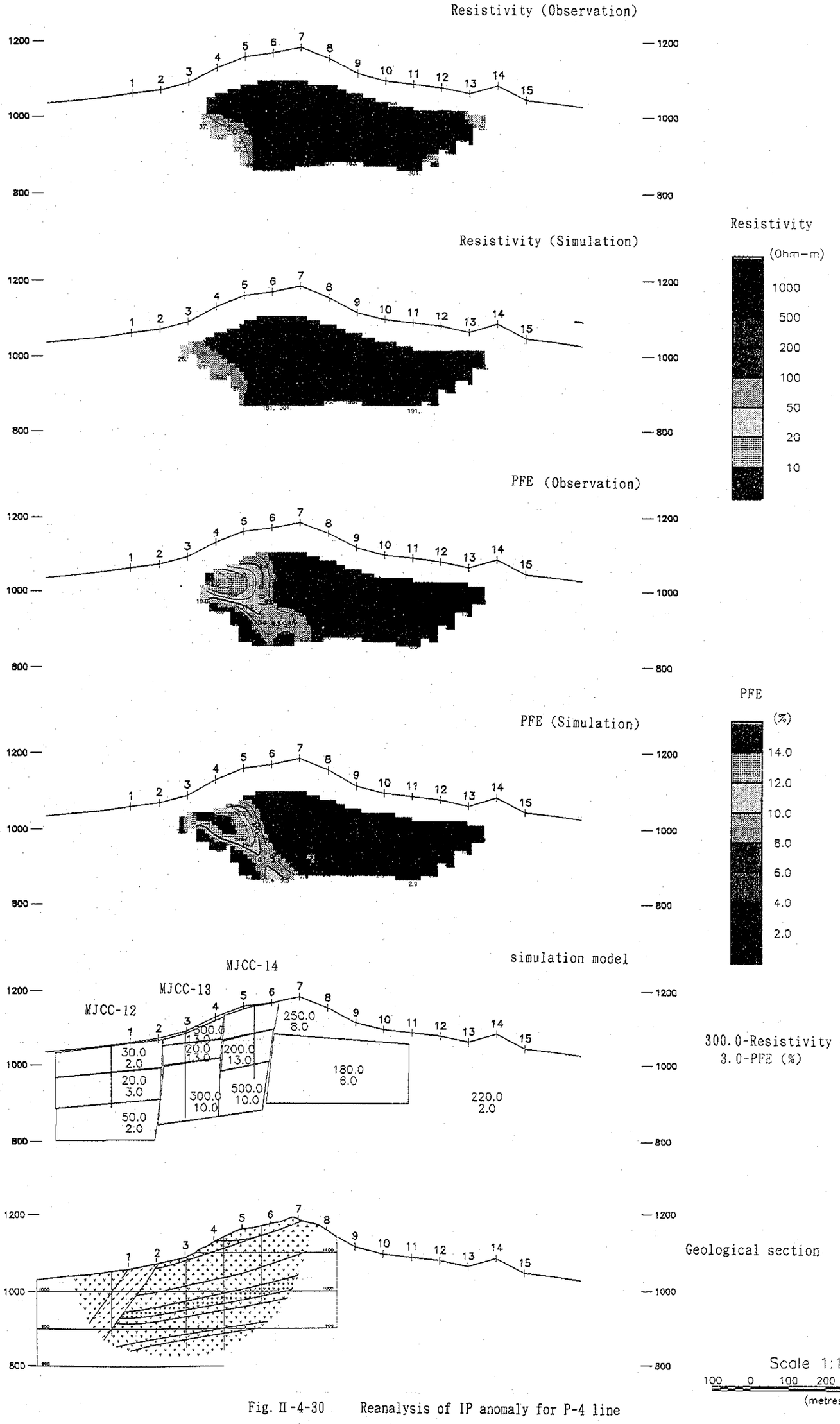

Fig. II-4-30 Reanalysis of IP anomaly for P-4 line

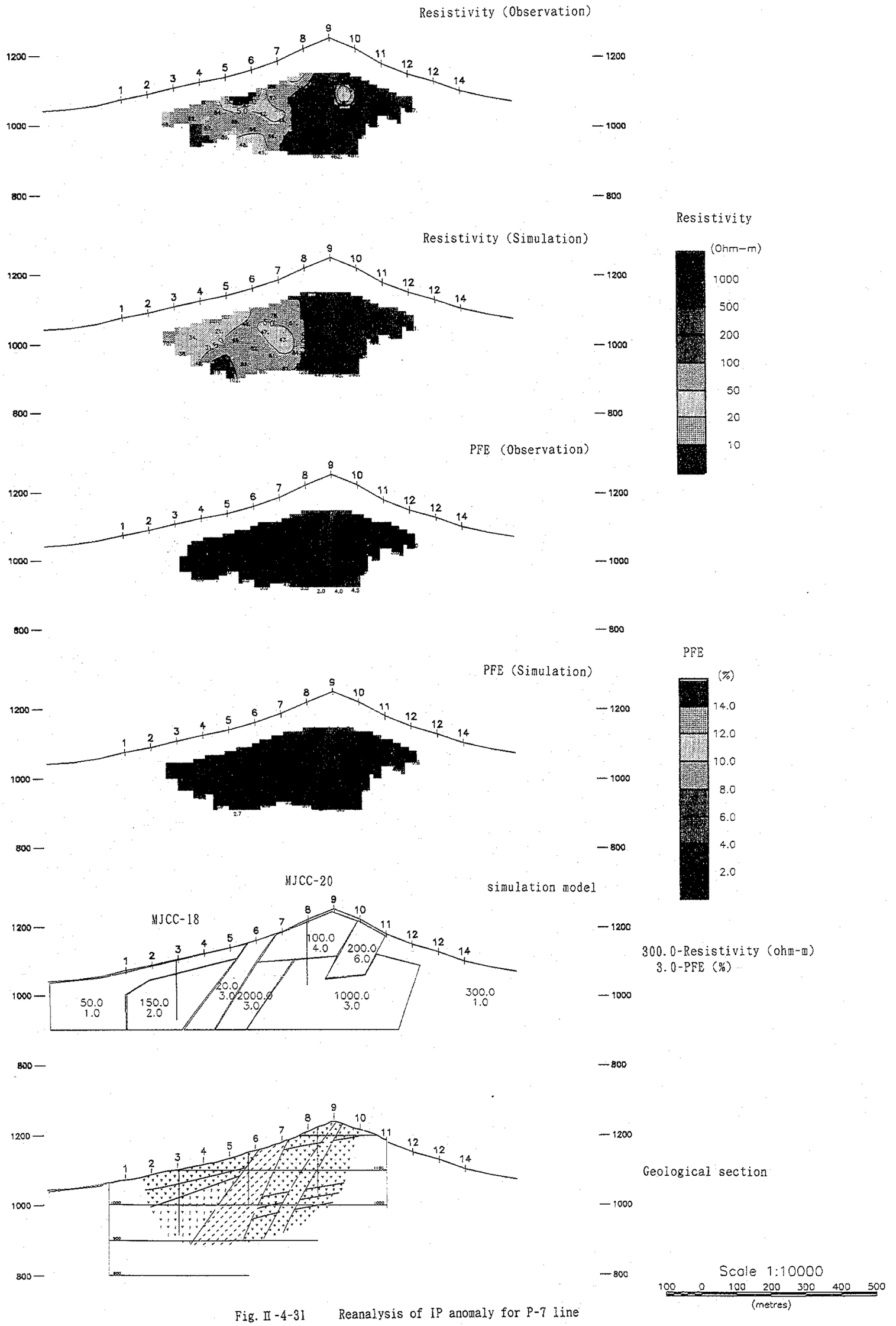

Fig. II-4-31 Reanalysis of IP anomaly for P-7 line

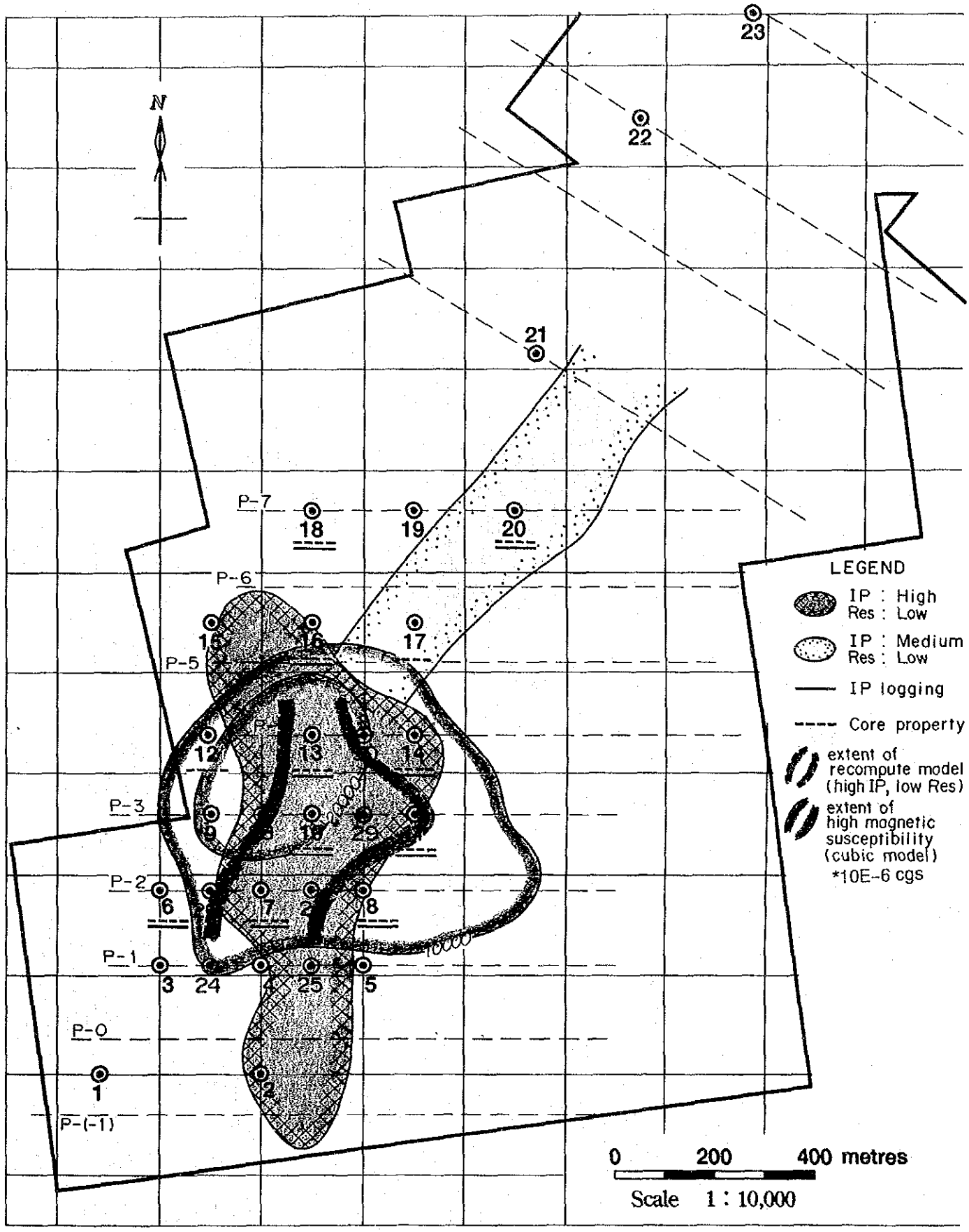

Fig. Ⅱ-4-32 Reanalysis of IP and Magnetic anomaly

4-3-4 Correlation among physical property of each drill holes

In order to investigate the cause of abnormally high IP with low resistivity as detected for the field IP survey, here we study the correlation among the physical property of each drill holes. The features of correlation among the physical property of each drill holes are as described below.

(MJCC-6): Fig. II-4-33

* Positive correlation is noted between IP and resistivity.
* Positive correlation is noted between IP and magnetic susceptibility.
* Positive correlation is noted between resistivity and magnetic susceptibility.
* Positive correlation is noted between magnetic susceptibility and total iron content.

From the above data, the following are pointed out:

* **Magnetite is considered as a possible cause of high IP value.**

The variety of resistivity is controlled by the magnetite content. Iron mostly consists of magnetite.

(MJCC-7): Fig. II-4-34

* Negative correlation is noted between IP and resistivity value.
* Negative correlation is noted between resistivity and total iron content.
* Negative correlation is noted between resistivity and insoluble copper content.

From the above results, the following is pointed out:

* **A drop in resistivity and high IP values seem to have been caused by chalcopyrite.**

(MJCC-8): Fig. II-4-35

* Positive correlation is noted between IP and resistivity value.
* Positive correlation is noted between IP and magnetic susceptibility.
* Positive correlation is noted between magnetic susceptibility and total iron content.
* Negative correlation is noted between resistivity and insoluble copper content.

From the above results, the following are pointed out:

* **IP and total iron content of this drill hole depend on the magnetite content. However, resistivity varies depending on the amount of chalcopyrite content.**

(MJCC-10): Fig. II-4-36

* Negative correlation is noted between IP and resistivity value.
* Negative correlation is noted between resistivity and insoluble copper content,

while positive correlation is noted between magnetic susceptibility and insoluble copper content.

* Negative correlation is noted between resistivity and total iron content/magnetic susceptibility.
* Positive correlation is noted between magnetic susceptibility and total iron content.

From the above results, the following are pointed out:

* **Resistivity of this drill hole depends on the chalcopyrite content.**
* **Total-iron contents depend on magnetite content.**
* **Because of high IP against low resistivity values, high IP values seem to have been caused by**

the involvement of sulfide (especially chalcopyrite).

(MJCC-11): Fig. II-4-37

* Negative correlation is noted between IP and resistivity value.
* Negative correlation is noted between resistivity and insoluble copper content.

From the above results, the following is pointed out:

* **Resistivity of this drill hole depends on the chalcopyrite content.**

(MJCC-12): Fig. II-4-38

* Positive correlation is noted between IP and resistivity.
* Two series of IP and resistivity relations are found, each with positive correlation between them.
* Positive correlation is noted between total iron content and magnetic susceptibility.

From the above results, the following is pointed out:

* **IP and total iron content of this drill hole depend on the magnetite content.**

(MJCC-13): Fig. II-4-39

* Negative correlation is noted between IP and resistivity value.
* Negative correlation is noted between resistivity and total iron content.
* Positive correlation is noted between metal conduction factors and total iron content.

From the above results, the following is pointed out:

* **IP and resistivity of this drill hole depend on the sulfide content (mainly chalcopyrite).**

(MJCC-14): Fig. II-4-40

* Three series of IP and resistivity relations are found, each with positive correlation between them.
* Two series of IP and magnetic susceptibility relations are found, each with positive correlation between them.
* Positive correlation is noted between total iron content and magnetic susceptibility.
* Three series of IP and total iron content relations are found each with positive correlation between them.

From the above results, the following is pointed out:

* **IP and total iron content depend on magnetite content. However, owing to high IP value against low resistivity values, they also seem to have been under the influence of sulfide (especially chalcopyrite).**

(MJCC-16): Fig. II-4-41

* Positive correlation is noted between IP and resistivity value.
* Positive correlation is noted between IP and magnetic susceptibility.
* Negative correlation is noted between resistivity and insoluble copper content.
* Positive correlation is noted between metal conduction factors and insoluble copper content.
* Positive correlation is noted between total iron content and magnetic susceptibility.

From the above results, the following are pointed out:

*** IP value of this drill hole depends on the magnetite content, while resistivity depends on the chalcopyrite content.**

*** Total-iron content depend on the magnetite content.**

(MJCC-17): Fig. II-4-42

* Two series of IP and magnetic susceptibility relations are found, each with positive correlation among them.

* Negative correlation is noted between resistivity and total iron content.

* Positive correlation is noted between metal conduction factors and total iron content.

From the above, the following is pointed out:

*** While IP value depends upon the magnetite content, resistivity value is under the influence of sulfide.**

(MJCC-18): Fig. II-4-43

* Positive correlation is noted between IP and resistivity.

* Two series of IP and magnetic susceptibility relations are found, each with positive correlation between them.

* Positive correlation is noted between magnetic susceptibility and total iron content.

* Two series of resistivity and magnetic susceptibility relations are found, each with positive correlation among them.

From the above results, the following is pointed out:

*** IP, resistivity and total iron content depend on the magnetite content.**

(MJCC-20): Fig. II-4-44

* Negative correlation is noted between resistivity and total iron content.

* Negative correlation is noted between resistivity and insoluble copper content.

* Positive correlation is noted between metal conduction factors and total iron content.

From the above results, the following is pointed out:

*** Resistivity of this drill hole depends on the chalcopyrite content.**

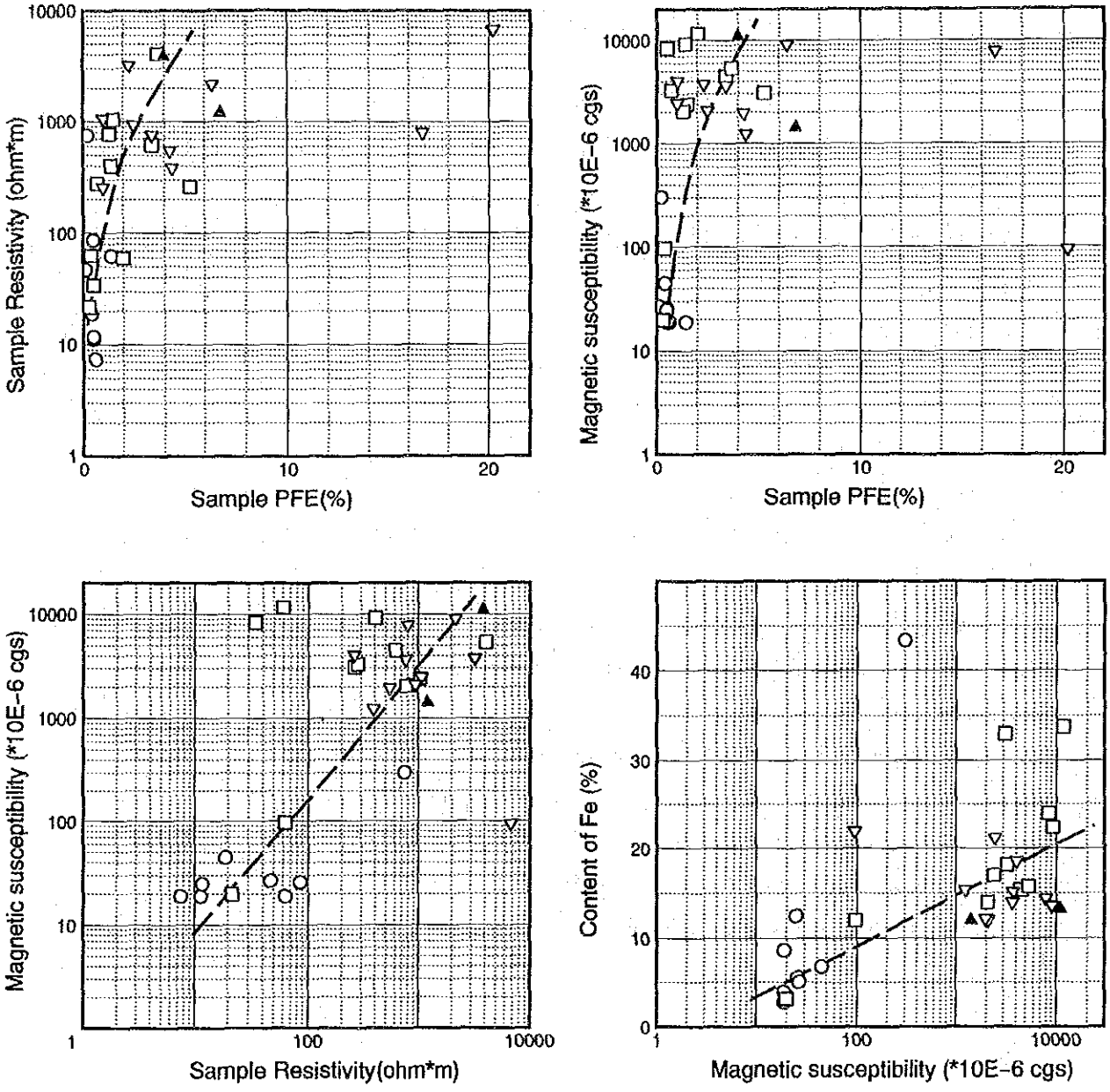

Fig. II-4-33 Correlation of physical property for MJCC- 6

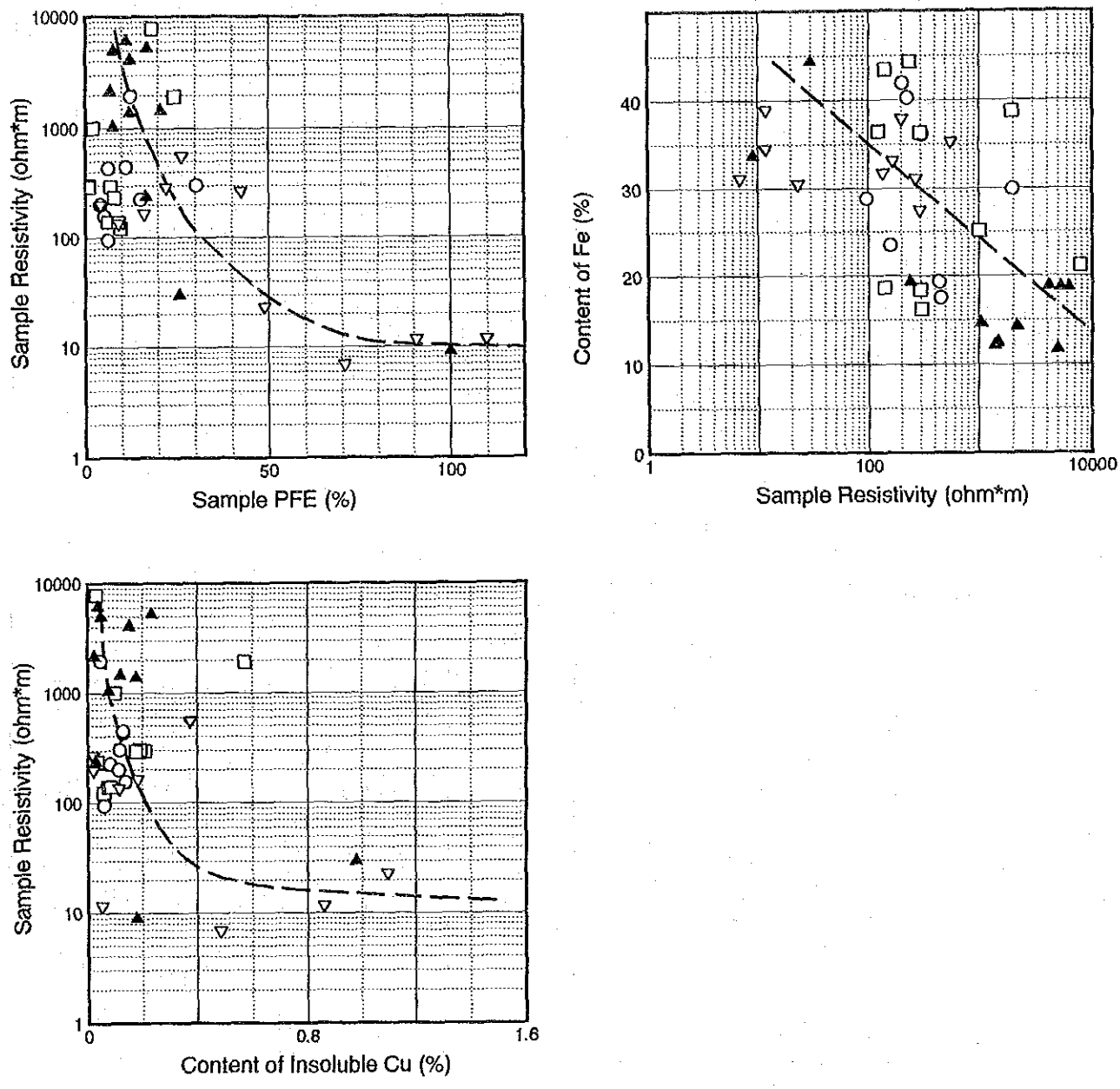

Fig. Ⅱ-4-34 Correlation of physical property for MJCC- 7

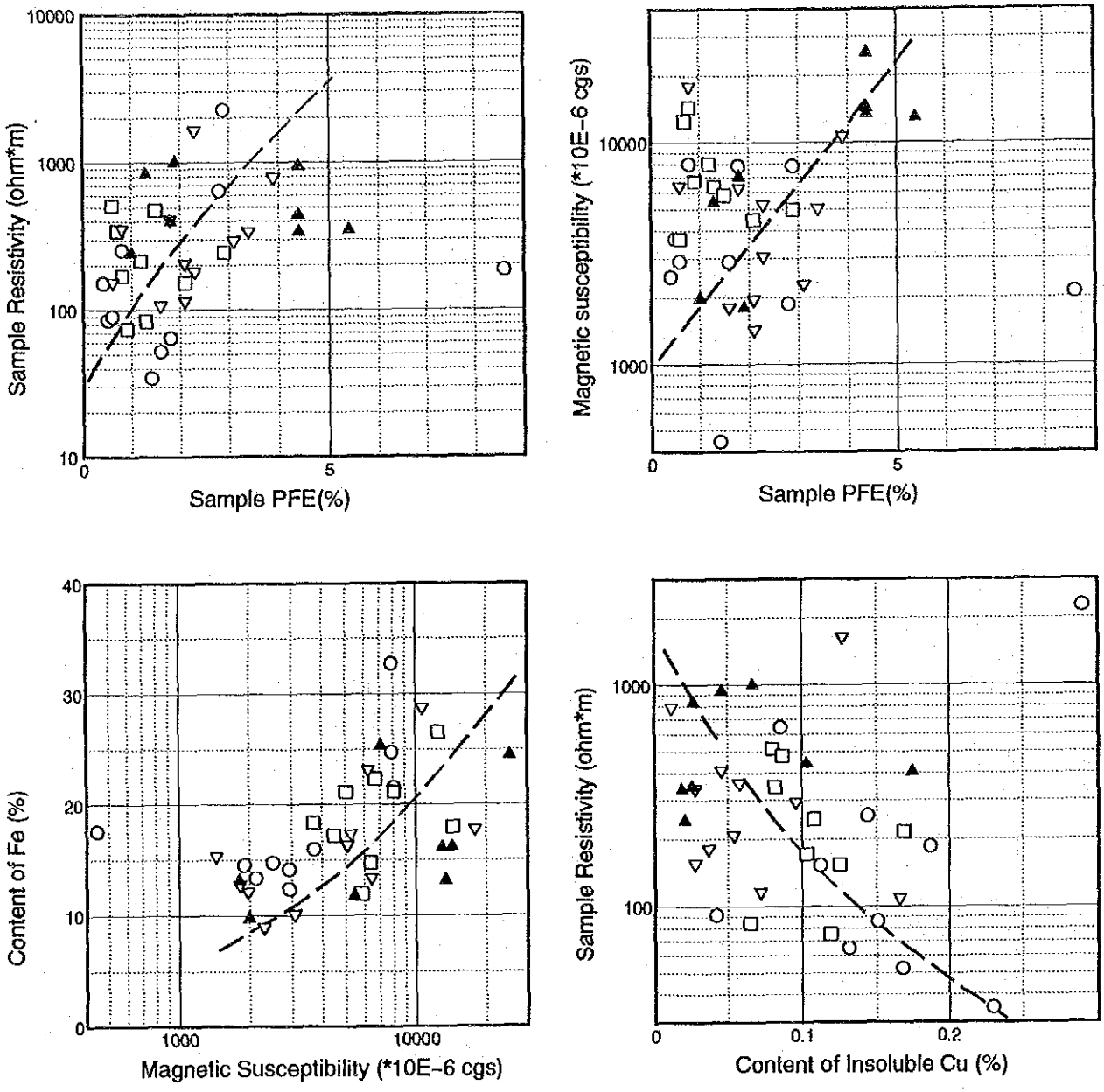

Fig. Ⅱ-4-35 Correlation of physical property for MJCC- 8

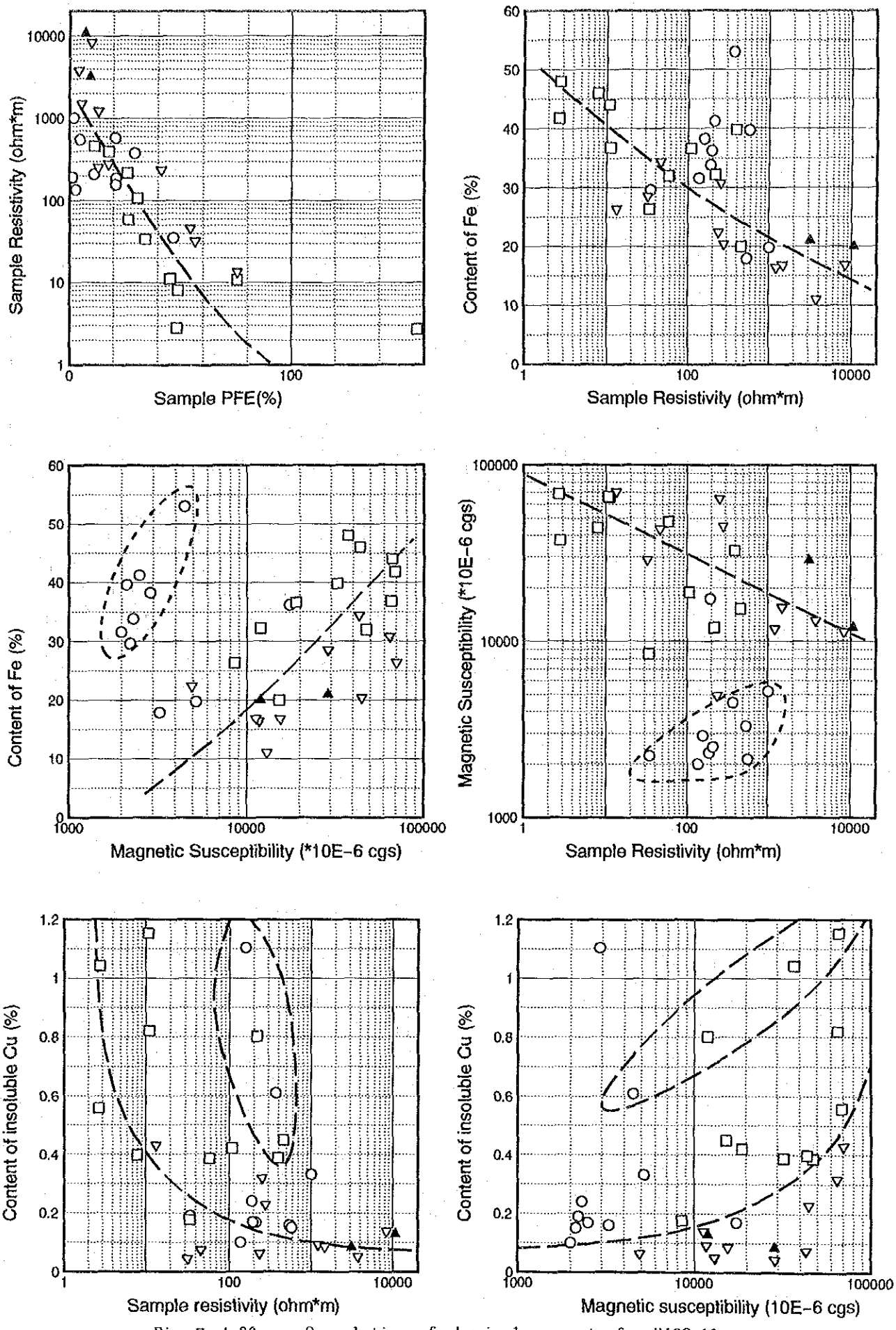

Fig. Ⅱ-4-36 Correlation of physical property for MJCC-10

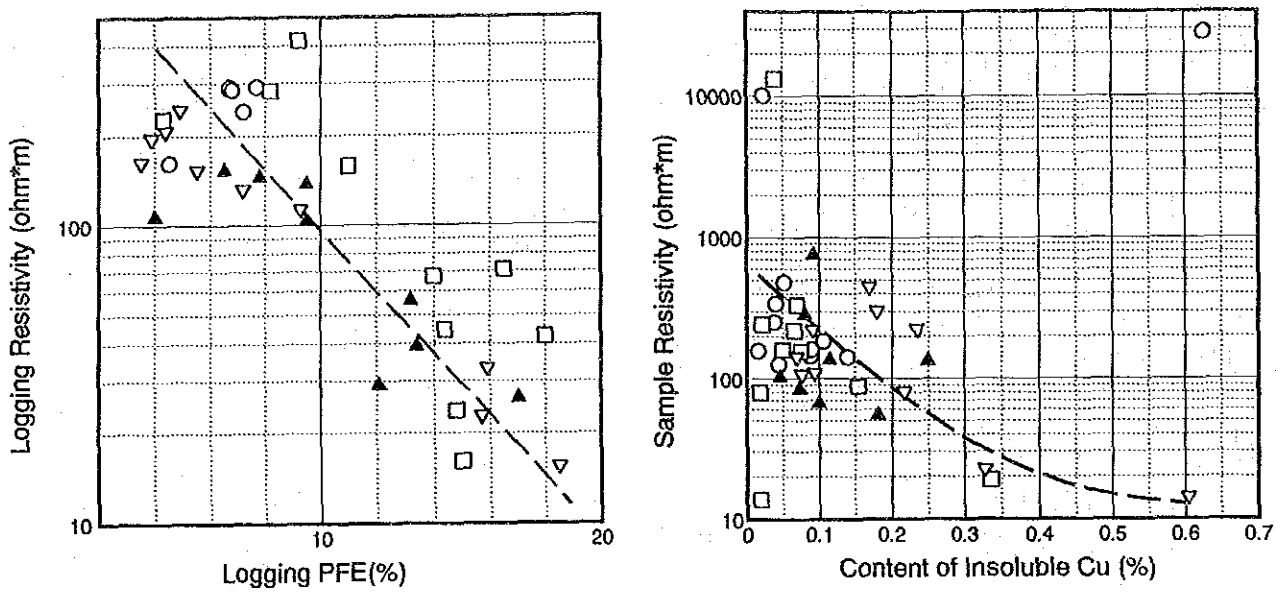

Fig. Ⅱ-4-37 Correlation of physical property for MJCC-11

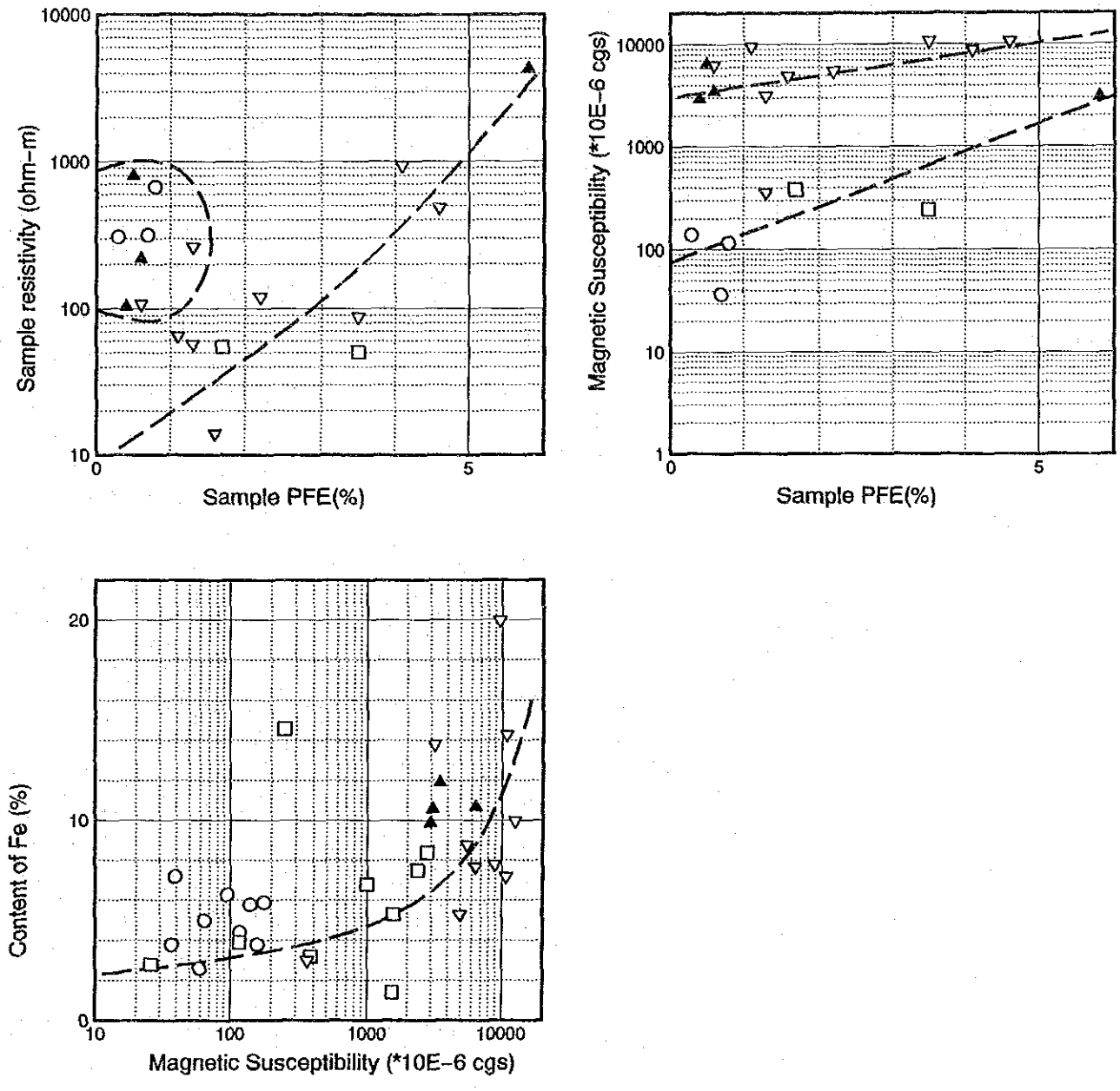

Fig. Ⅱ-4-38 Correlation of physical property for MJCC-12

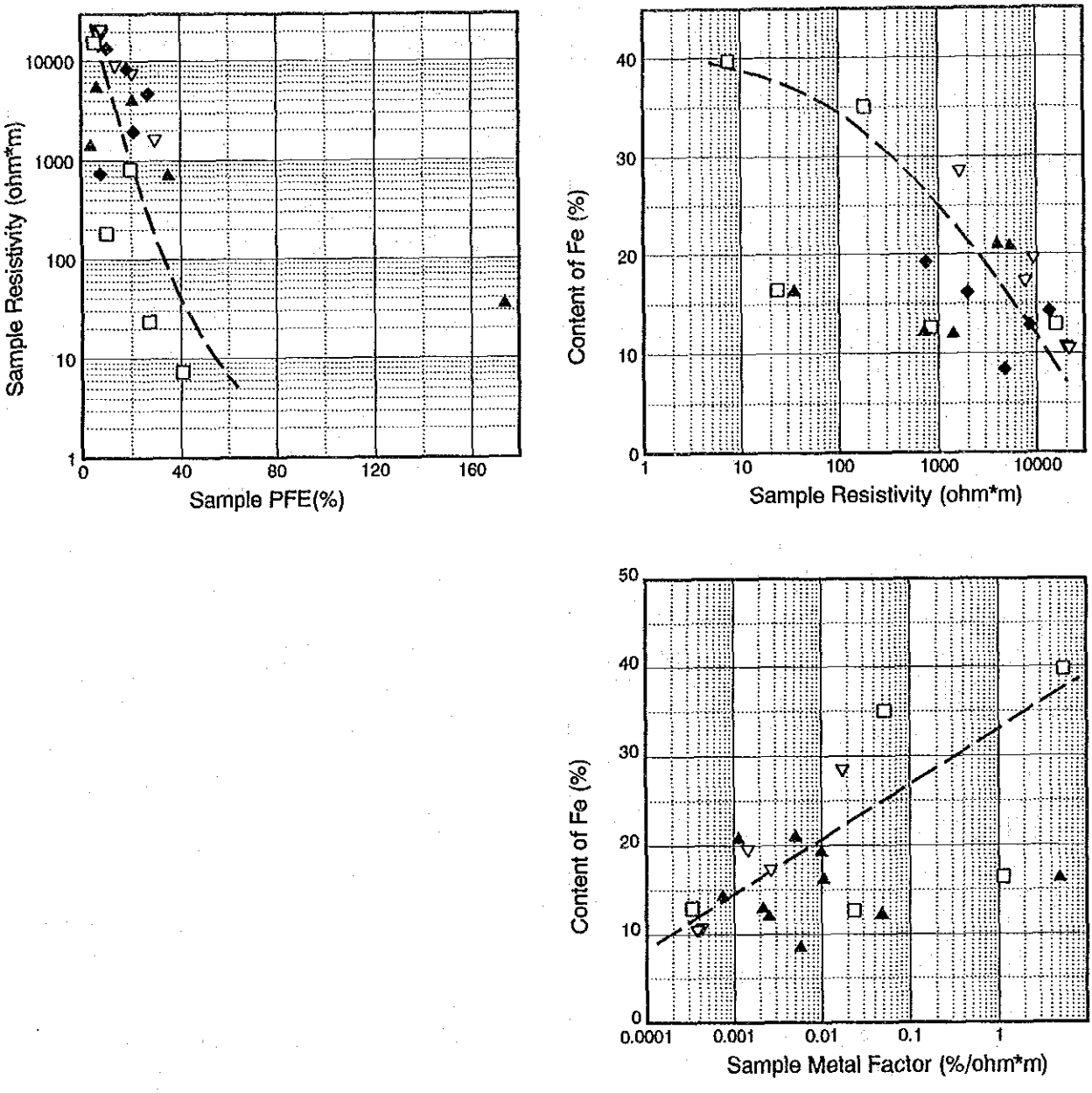

Fig. Ⅱ-4-39 Correlation of physical property for MJCC-13

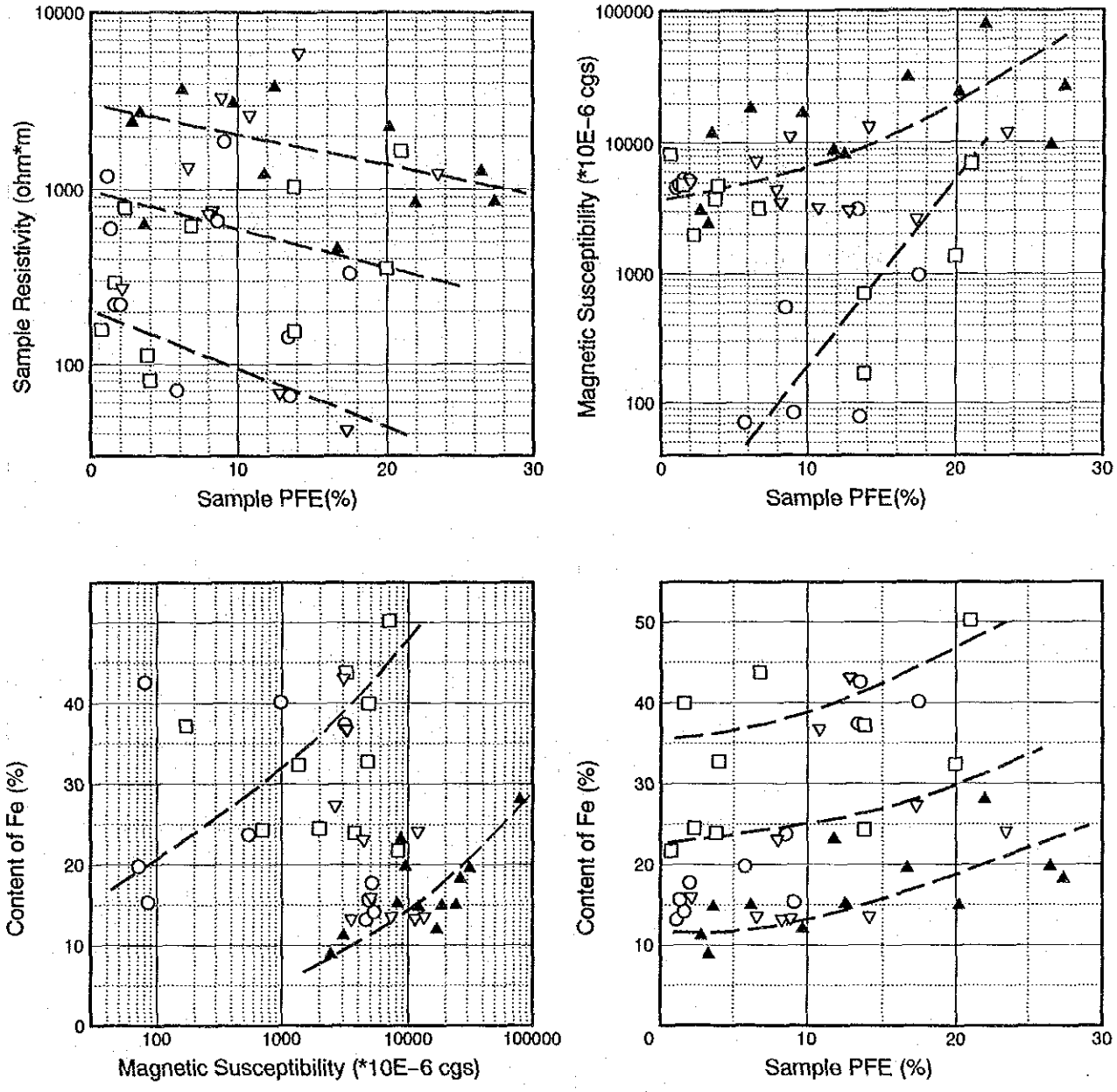

Fig. Ⅱ-4-40 Correlation of physical property for MJCC-14

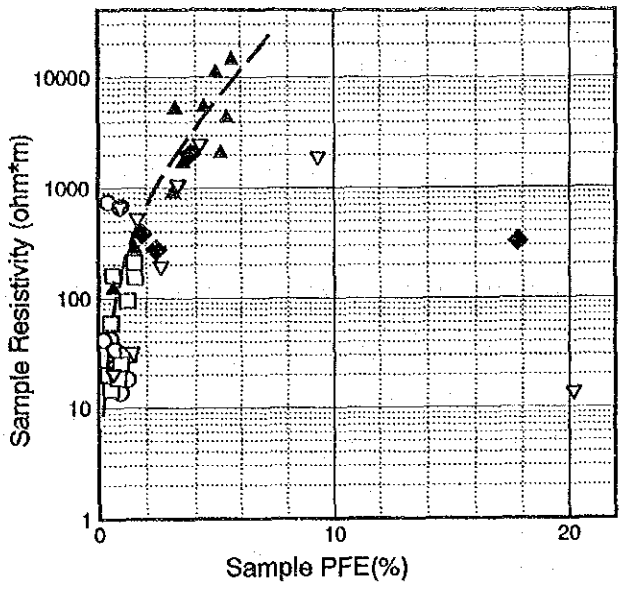

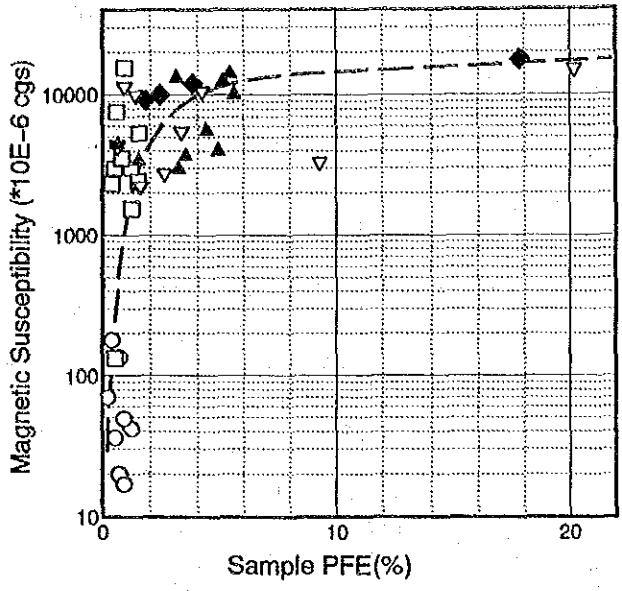

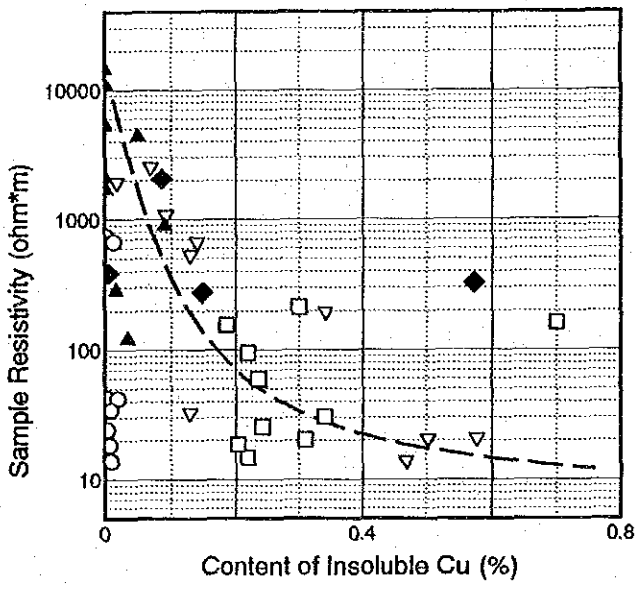

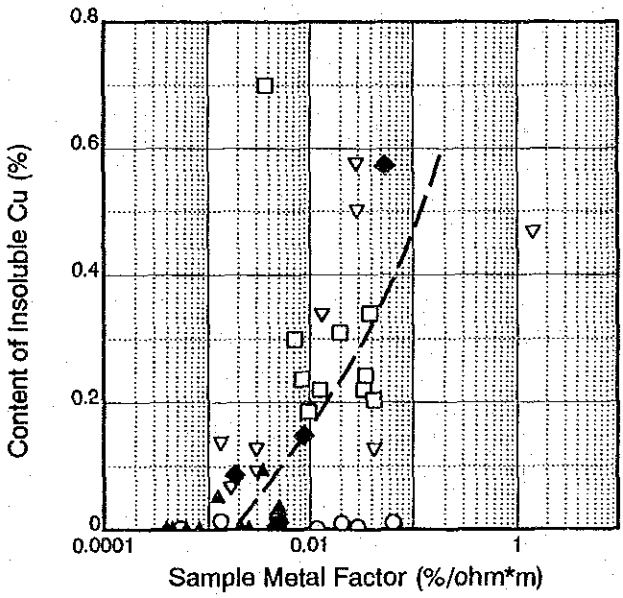

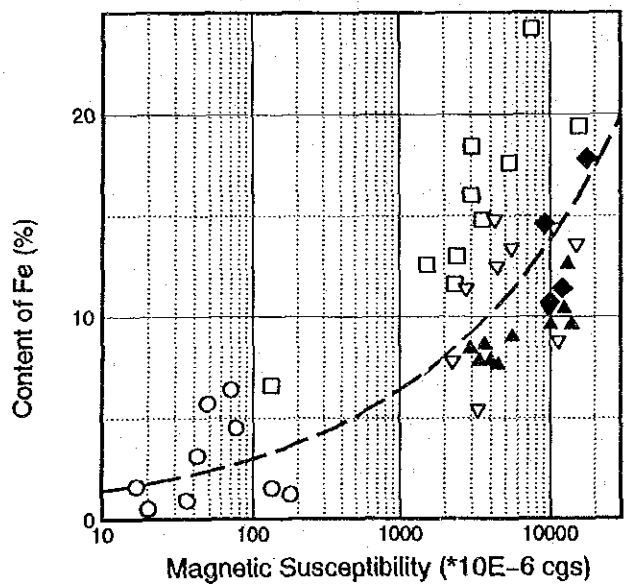

Fig. II-4-41 Correlation of physical property for MJCC-16

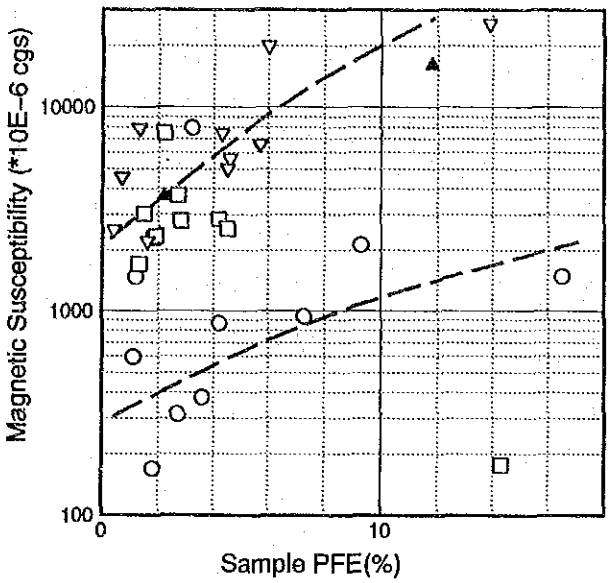

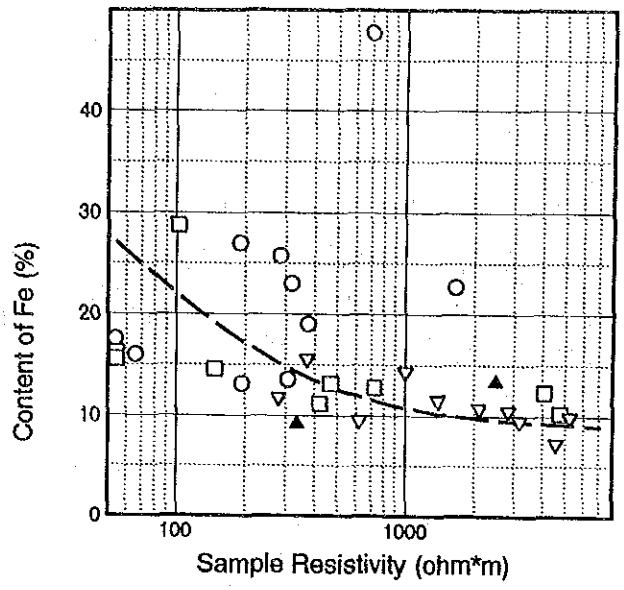

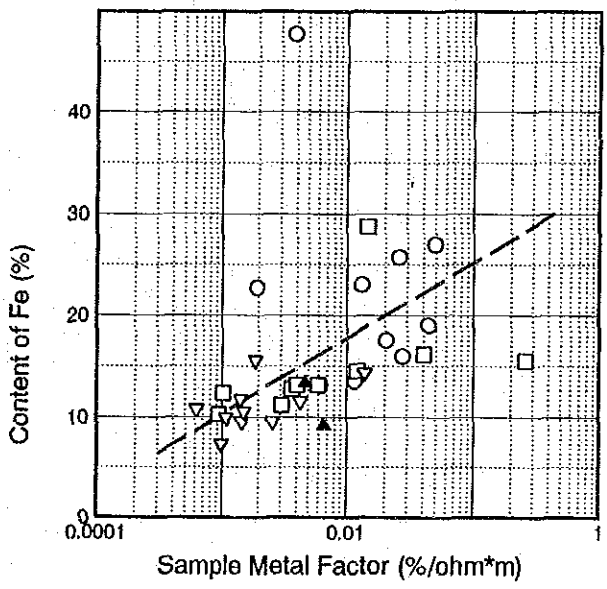

Fig. Ⅱ-4-42 Correlation of physical property for MJCC-17

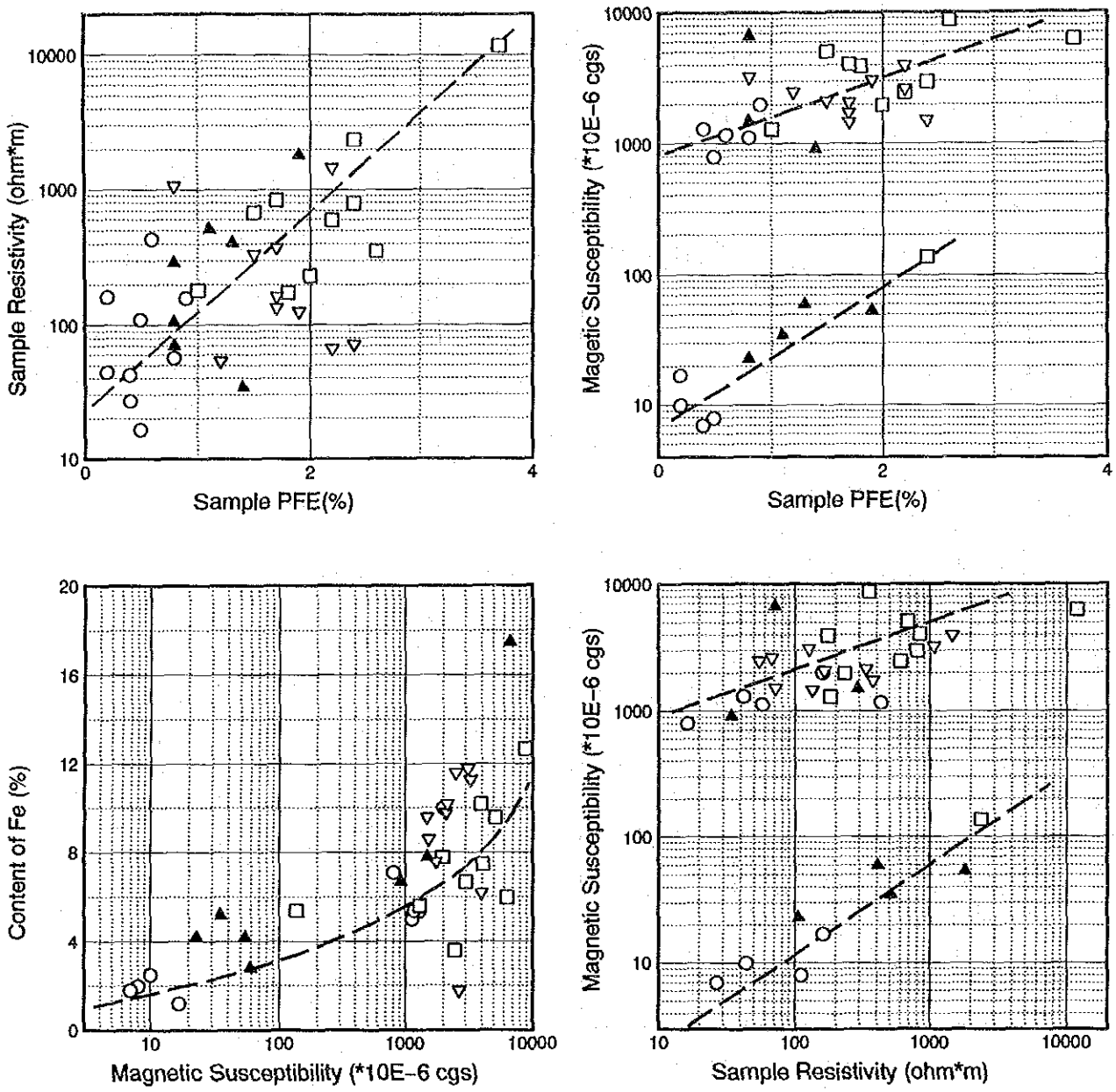

Fig. II-4-43 Correlation of physical property for MJCC-18

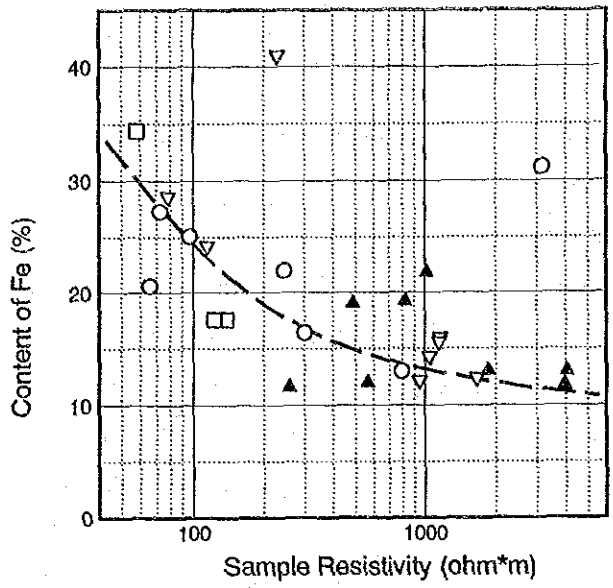

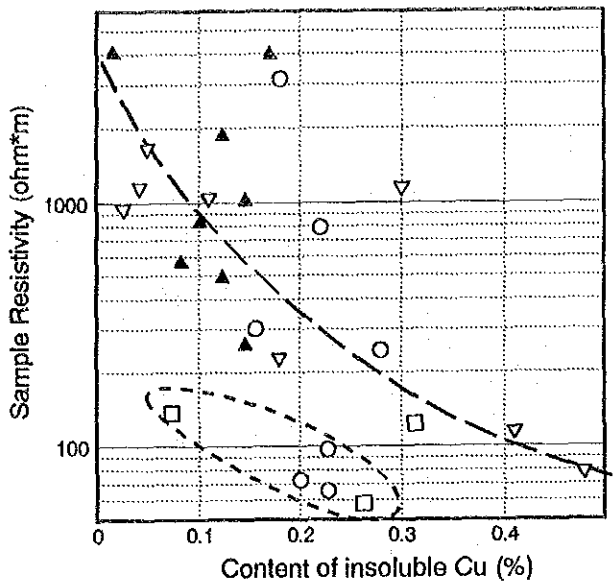

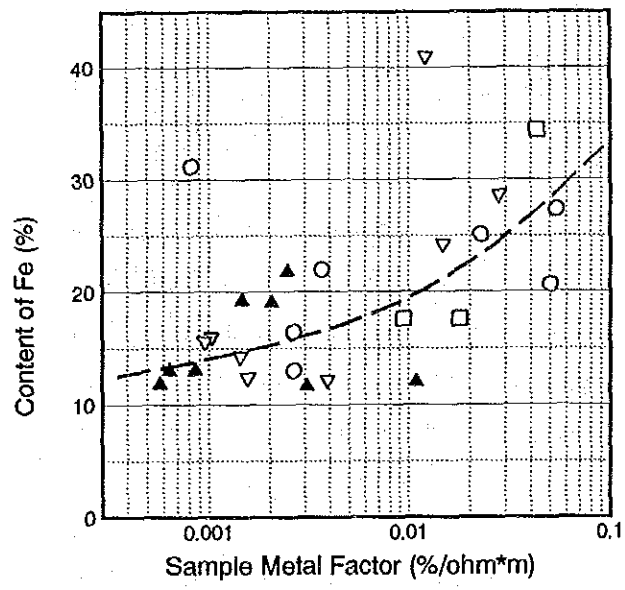

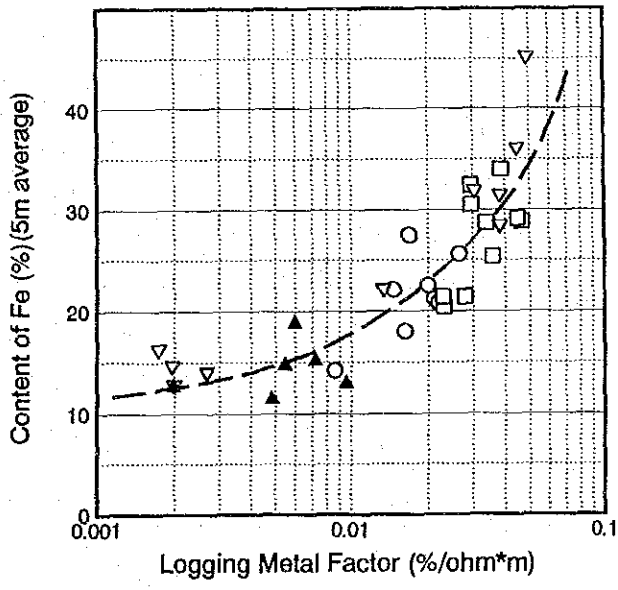

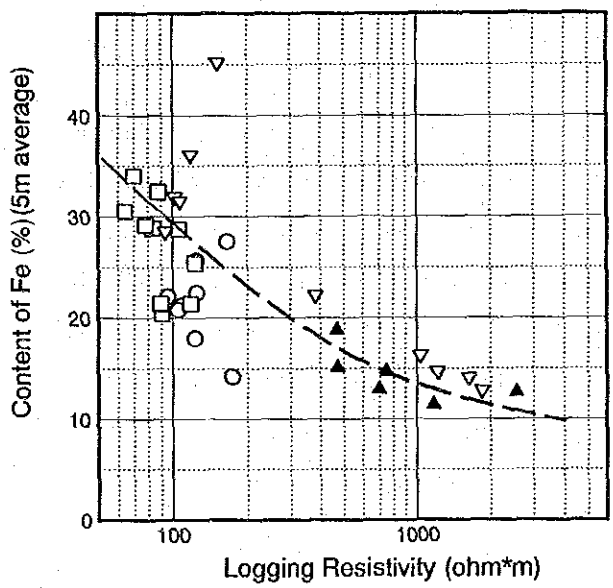

Fig. Ⅱ-4-44 Correlation of physical property for MJCC-20